Age-Sensitive Features for Detection of Muscle Fatigue using the High-Density Electromyogram

by

Bharath Krishnan

A thesis

presented to the University of Waterloo in

fulfilment of the

thesis requirement for the degree of

Master of Applied Science

in

Systems Design Engineering

Waterloo, Ontario, Canada, 2021

Author's Declaration

The contents of this thesis consist of material all of which I authored or co-authored: see Statement of Contributions included in the thesis. This is a true copy of the thesis, including any required final revisions, as accepted by my examiners. I understand that my thesis may be made electronically available to the public.

Statement of Contributions

The publications that are associated with the work presented in this thesis are as follows:

I. **Krishnan B**., Zanelli, S., Boudaoud, S., Scapucciati, L., McPhee, J., Jiang, N. "Age-sensitive High Density Surface Electromyogram Features for Detecting Muscle Fatigue Using Core Shape Modelling" (Submitted for publication)

The research associated with this paper was conducted at the University of Waterloo by Bharath Krishnan, Léa Scapucciati and Serena Zanelli under the supervision of Dr. Ning Jiang, Dr. John McPhee, and Dr. Sofiane Boudaoud. Léa Scapucciati and Serena Zanelli were responsible for the study design and participant recruitment. Bharath Krishnan and Serena Zanelli were primarily responsible for the coding and data analysis. Bharath Krishnan wrote the draft manuscripts which all co-authors intellectually contributed on.

Abstract

The processes behind fatigue development within the muscles have been a topic of interest for exercise scientists for decades. This is because fatigue is one of the primary reasons for a decrease in performance and increase in likelihood of injury during exercise[1]. Typically, muscle fatigue is detected through modifications of the amplitude and spectral characteristics of a surface electromyogram (sEMG), or the variability of torque signals recorded throughout a sustained contraction. However, the behaviour of these parameters with the generation of fatigue depends on a variety of factors. One major factor is age, where the age-related loss of muscle fibers, and changes in neuromuscular system impact how muscles adapt to and develop fatigue. The purpose of this study was to examine age-sensitive High Density Surface Electromyogram (HD-sEMG) features and investigate the effect of spatial filter type on intramuscular coherence analysis in fatigue detection. Fatiguing submaximal isometric contractions of the bicep brachii was performed by eight young (24.40 ± 2.42 years) and five elderly (72.90 ± 2.21 years) males, while HD-sEMG recorded signals from the biceps brachii and a dynamometer recorded torque signals. The task was performed at 20% maximal voluntary contraction (MVC). From the HD-sEMG signals, the mean intramuscular coherence was calculated in the alpha (11-15Hz), beta (16-29Hz), and gamma (30-50Hz) frequency bands each of which stems from different neurological origins. Statistical differences were only found in the alpha ($p=0.0006$), and beta ($p=0.0207$) bands between the pre- and post-fatigue conditions of the young group. Furthermore, a correlation between mean coherence and torque variability during the final 25% of the contraction before task failure revealed that both the age groups had positive correlation in the alpha band. Different correlations were found in the beta and gamma bands, with positive correlations being observed in the elderly group and negative correlations in the young group. These results suggest that age-related changes in the corticospinal pathway exist causing the elderly to be less fatigable when compared to the young

population. This proposes that the introduced intramuscular coherence analysis can be used to obtain fatigue related features from HD-sEMG signals that are age-sensitive.

Acknowledgements

I would first like to express my gratitude to my supervising professor Dr. Ning Jiang for the immeasurable amount of guidance and patience he provided throughout my work on this project. He assisted in every step during my MASc providing me with not only financial support, but with motivational support to continuously challenge myself regarding the topics surrounding my work. This was especially apparent when I had to switch thesis topics due the COVID-19 pandemic thereby extending the length of my MASc program. He was extremely supportive and provided me with the resources to do my research remotely at home whilst taking little away from the overall experience.

I would also like to extend thanks to Dr. Sofiane Boudaoud for providing me with invaluable data to pursue my chosen thesis topic as well as guidance regarding the manuscript produced during this project.

Appreciation is also owed to the past and present lab members of the eBionics Lab, especially Andrew Smiles, Aravind Ravi, and Benjamin Lambert. These members both knowingly and unknowingly assisted me with the overall structure, formatting, and organization decisions during the writing phase of my thesis.

I would also like to thank my family as without their moral support, none of my work would be possible.

Table of Contents

List of Figures

List of Tables

List of Abbreviations

ARV: Average Rectified Value

BMI: Body Mass Index

BP: Bipolar

CoV: Coefficient of Variation

F25: Final 25% of the sustained contraction

HD-sEMG-: High Density Surface Electromyography

I25: Initial 25% of the sustained contraction

LA: Laplacian

RMS: Root-Mean-Square

sEMG: Surface Electromyography

MDF: Median Frequency

MNF: Mean Frequency

MP: Monopolar

MU: Motor Unit

1. Introduction

Muscle fatigue, and the underlying mechanisms responsible for the phenomenon have been one of the primary focuses in the fields of sport, exercise, rehabilitation and ergonomics [2]. Understanding these mechanisms is critical in the improvement of performance and/or prevention of musculoskeletal injury. A major difficulty in understanding the development of muscle fatigue is considering the various factors that may affect the processes behind fatigue generation, such as aging. Generally, it is accepted that advanced aging causes changes in the musculoskeletal system, resulting in a loss of muscle mass and strength[3], [4]. However, it is still relatively unclear how the process of aging changes the muscles resistance to fatigue. In recent years, it has become widespread in the literature to evaluate muscle fatigue using surface electromyography (sEMG) as changes in the signal can provide information about biochemical and physiological changes in the muscle [5]. However, a single pair of sEMG electrodes provide limited spatial coverage, and therefore lacks the ability to capture the activity across a muscle and a muscle group, potentially missing vital spatial information about the muscles' activity. To address this, High-Density sEMG (HD-sEMG) technology can be used as it accounts for both spatial and temporal characteristics of the signal allowing for a broader assessment of muscle activity [6]. Another issue associated with the poor spatial coverage of conventional sEMG is that it typically picks up activity of motor units (MUs) in the electrodes' vicinity, which increases the difficulty to make conclusions about specific muscles/MUs. The usage of HD-sEMG allows for the construction of different electrode configurations which can be used to implement spatial filters to help isolate motor units within the muscle. As muscle fatigue progresses, the degree of synchronization between firing times of simultaneously active MUs is believed to increase [7], [8]. Coherence analysis can be used to quantify this correlated MU activity, however using this analysis whilst utilizing the increased

spatial information provided by the HD-sEMG remains largely unexplored. The exploration of coherence whilst leveraging the spatial advantages of the HD-sEMG may give more insight into how fatigue develops within the muscle and more accurate detection of muscle fatigue.

For HD-sEMG data from the young and elderly subjects that underwent a fatiguing contraction, there are the following main objectives of this thesis:

I. Evaluate the ability of different spatial filter electrode configurations to detect fatigue related differences in a) conventional EMG features and, b) mean coherence within, and between the different age groups.
II. Compare the evolution of force steadiness and mean coherence in each frequency band.
III. Examine age-related differences in muscle fatigue generation

2. Background

2.1. Muscles and Muscular Fatigue

Muscles that are continuously and/or intermittently activated eventually show a gradual decline of performance. This process is known as muscle fatigue. In the fields of sports and rehabilitation, this phenomenon is one of the most prevalent mechanisms that result in an increase in likelihood of injury and decrease in overall task performance. Fatigue can be split into two categories based on where it originates from: central fatigue which originates from the central nervous system (CNS) and peripheral fatigue which originates from the peripheral nervous system (PNS) [8].The purpose of this section of the review is to 1) Examine the underlying physiology of muscles, 2) Examine the physiological processes underlying muscular fatigue and its impact on muscle function and 3) Understand how age affects the physiology of the muscle and how it impacts the generation of muscle fatigue.

2.1.1. Muscles

Muscles are one of the components that make up the musculoskeletal system, where its primary role is for maintaining body weight, posture and assisting in movement [9]. All the muscles in the human body can be split into 3 distinct groups: skeletal, cardiac, and smooth muscles. The type of muscle primarily responsible for movement is skeletal muscle, which attaches to the bone via tendons and work together to produce movement. Each skeletal muscle is made up

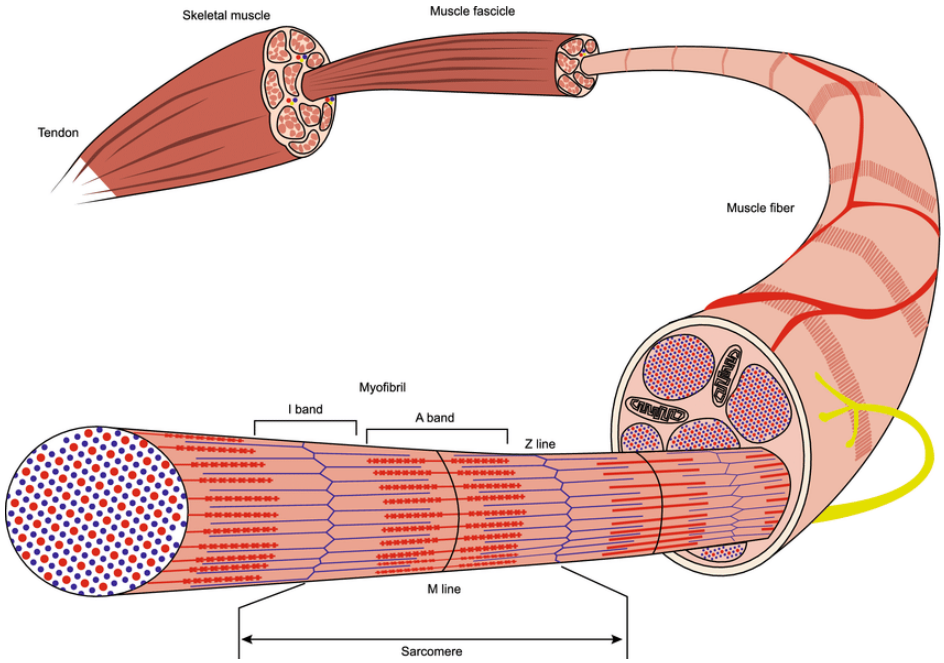

Figure 1: Skeletal muscle anatomy. Taken from [124]

of thousands of muscle fibers wrapped together by connective tissue sheaths [10]. These muscle fibers are typically classified as Type I (slow-twitch) or Type II (fast-twitch) and these fibers are bundled together in the muscle to form fascicles [11]. Each muscle fiber in the fasciculi contain numerous myofibrils which each contain several myofilaments, as seen in Figure 1 .

Myofibrils are bundled together in a striated pattern forming sarcomeres, which is known as the fundamental contractile unit of the muscle [10]. Within the sarcomeres, the actin and myosin myofilaments play the most significant role for contraction. Contraction of the muscle is elicited

by means of action potentials from the CNS which triggers the release of actin filaments, allowing for myosin binding and muscle contraction [12] .

Action potentials that elicit contractions are delivered to the muscle through signalling from alpha motor neurons. One of these motor neurons can innervate several muscle fibers, forming a motor unit (MU). The number of MUs activated generally depend on the required force, where maximal amounts of force require maximal amounts of MUs. Although maximal MUs are activated, all available MUs are not simultaneously activated to prevent complete muscle fatigue [11]. The size of the MU is indicative of its function, with smaller MUs being responsible for precise control of a muscle and larger MUs are responsible for general/simple movements [11]. A twitch occurs when a single action potential from a motor neuron produces a single contraction in

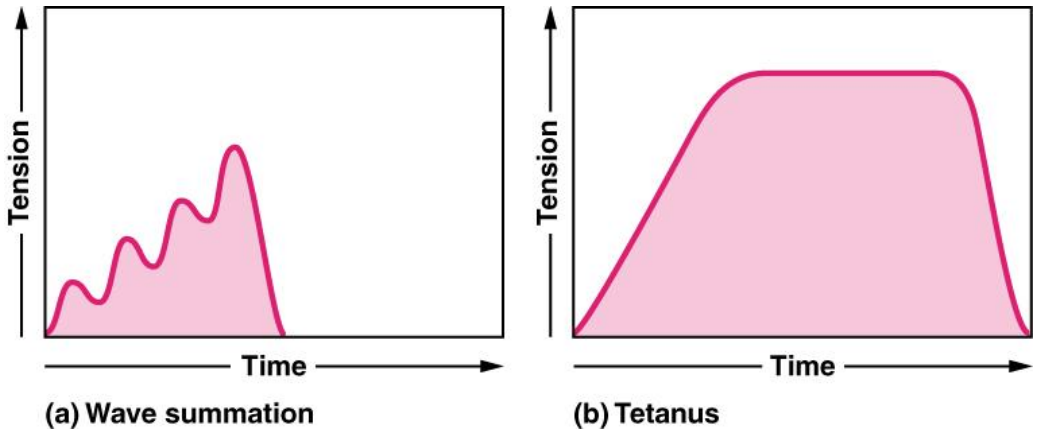

Figure 2: Temporal summation in the muscle. Taken from [11].

the muscle fibers it innervates. The resulting force of a muscle's contraction can be modulated through descending neural drive applied to the motor unit pool of the muscle. An increase in descending drive would result in a general increase of activating frequencies of the motor units in the pool. Consequently, the force twitches of the motor unit would occur in faster succession. This leads to wave summation, where a new force twitch is superimposed on the previous twitch, resulting in a stronger over all force output. The temporal frequency can continue to increase

reaching a state of incomplete tetanus and then eventually complete tetanus, where the relaxation phase completely disappears between twitches. However, complete tetanus rarely occurs, and it cannot be sustained as it eventually leads to muscle fatigue.

Motor units are recruited based on the Henneman's size principle, which dictates that during a contraction MUs that have the smallest fibers are activated first [13]. When a contraction first starts, the smallest and most excitable MUs are activated, then as the contraction is sustained, larger and larger MUs are recruited. The muscle fibers themselves can be split into two different categories. Type I fibers are characterized by low force twitch and speed but are highly fatigue resistant, whereas type II fibers generally have capabilities of high force twitch but have lower fatigue resistance.

2.1.2. Muscle Fatigue: Central and Peripheral Factors

From a skeletal muscle's perspective, fatigue can be defined as the decline of a muscle's ability to produce force or power in response to the same level of target force or power level. Several physiological processes that contribute to the muscle fatigue start at the beginning of a sustained contraction and continues until the contraction is completed or failed. Once the contraction has finished, fatigue related changes in the muscle during the contraction gradually reverts to its original state [14]. The accumulation of muscle fatigue is not solely due to processes within the muscle. In fact, there are two systems that influence the generation of muscle fatigue, as such they are split into two categories: central fatigue and peripheral fatigue. In this case, central fatigue refers to fatigue caused by processes of spinal and/or supra-spinal sources whereas peripheral fatigue stems from the peripheral nerves, neuromuscular junction and muscles [15].

Central fatigue is an important aspect of muscle fatigue as processes with the CNS reduce the neural drive to the muscle causing a decline in performance, despite conscious effort to maintain the output of the muscle [16]. Specifically, the CNS via central neurotransmitters such as dopamine play a key role in the activation and inhibitory responses of motoneurons during fatigue [17]. This is one of the main mechanisms that ultimately activates MUs for force production. When the CNS elicits the repetitive activation of motoneurons during a sustained contraction, changes in the intrinsic properties of the motoneurons occur[16]. These changes could result in a reduction in the ability to respond to excitatory synaptic input, thereby decreasing the ability to sustain a force. Sensory neurons innervating skeletal muscle also performs a critical role in the development of central fatigue. These neurons, namely group III and IV muscle afferents, are responsible for conveying information to the CNS about nociceptive, non-nociceptive, mechanical, chemical and thermal events that take place within the muscle [18]. Feedback from these muscle afferents during a fatiguing task results in the impairment of spinal motoneurons, causing a reduction in muscle activation[16].

Peripheral fatigue refers to the decline in force generating capacity due to factors originating in the muscle itself rather than the CNS [7] . This is typically characterized by the depletion of energy stores, accumulation of by-products and/or the impairment contractile mechanisms within the muscle [19]. Specifically, peripheral fatigue impairs contractile mechanisms from the neuromuscular junction (where motor neuron connects to muscle fibers) to where the muscle connects to the tendon (muscle-tendon complex) both electrochemically and mechanically [20]. Major electrochemical mechanisms of the muscle that are affected are the action potential synaptic transmission, propagation of action potentials (conduction velocity) across the sarcolemma, and the excitation-contraction coupling [20]. From a mechanical

perspective, peripheral fatigue influences force transmission between the muscle and tendon by altering the stiffness and viscoelasticity of the muscle-tendon complex and surrounding tissues [20].

2.1.3. Muscle Fatigue and Aging

As an individual ages, modifications occur within the neuromuscular system which may result in changes of the size, shape and fiber composition of skeletal muscles [3], [4]. This age associated loss in muscle mass and strength is due to increased fat infiltration, which is commonly referred to as sarcopenia [21]. Epidemiological studies estimate that sarcopenia is prevalent in 5-15% of elderly people aged 60-70 years old but this number rises to 11-50% in those aged 80 or above [22]. The loss of muscle mass associated with age may involve a decrease in the number of muscle fibers, specifically type I and II. As both fiber types have different resistances to fatigue, the loss of these muscle fibers in the elderly may result in a different response to fatigue. In fact, one study found that the elderly group had 24% less type II muscle fibers, and 20% less mean muscle fibers in the biceps brachii when compared to the young [23]. Similarly, a study on the number of fibers within the vastus lateralis reported 50% less in number of fibers and 24% reduction in type II muscle fibers [24]. The reduction in type II fibers suggest that elderly produce contractions with less strength but in turn also fatigues more slowly when compared to the young.

Throughout the literature, it has been seen that healthy elderly subjects are typically less fatigable than young adults in both maximal and submaximal contractions [25]. This behaviour between young and elderly subjects are consistent between different muscle groups [26]–[28], sexes [28], [29], intensities [28], as well as when subjects of both age groups are matched for strength [30]. However, some studies reported no difference in fatigue or the elderly being more fatigued [31]–[33]. The inconsistencies in these results could be attributed to the contraction type

or methodology implemented, with studies utilizing dynamic contractions typically reporting the elderly being more susceptible to fatigue.

2.2.Electromyographical Signal Processing and Properties

Currently, surface electromyography (sEMG) is one of the most widely used non-invasive modalities to record muscle fatigue and muscle activity in general [5]. EMG works by detecting the electrical potential generated by muscle fibers through the skin. However, the recorded signal's amplitude is considerably weak at 1-10 mV [34]. The frequency of the signal is between 0-500Hz with majority of the energy being between 50-150 Hz [34], [35]. It also is able to capture changes in neuromuscular and morphological properties that occur during muscle fatigue through modifications in its time-domain and spectral parameters [5]. In contrast to sEMG, HD-sEMG adds a spatial dimension to the signal by arranging multiple electrodes in a two-dimensional grid over a muscle, thereby enhancing the spatiotemporal resolution of a typical sEMG signal. Each electrode on the grid are made of an electrically conductive material (typically Au, Ag, AgCl) , have a diameter of 3-5mm and have interelectrode distances between 5-10mm to avoid aliasing [36].

The usage of HD-sEMG allows for a more representative view of the muscle during a contraction, providing additional information about the activation, fiber heterogeneity and distribution of a muscle [37]. Another advantage of HD-sEMG is that it allows for the implementation of spatial filters using different electrode configurations. This is important as sEMG in general has a large pick-up volume, meaning the activity of multiple muscles far from the electrode can potentially be reflected in one signal [38]. Leading to one of the most prominent obstacles in sEMG analysis, crosstalk, which is defined as the signals observed from target muscles that are contaminated by different muscles [38]. This is unfavorable in EMG studies as conclusions

cannot be made about specific areas/muscles if signals from other areas are also being recorded. Spatial filtering can be used to reduce the effect of crosstalk as well as other unwanted components such as movement artifacts [39]. Among the different spatial filters, Bipolar (BP) and Laplacian (LA) are commonly implemented to isolate wanted parts of the signal [40]–[42]. BP is one of the most applied spatial filters in sEMG studies, for which the difference between the signals recorded from two adjacent electrodes, typically 1-3cm apart, along the muscle fiber direction are calculated [43]–[46]. LA acts as a spatially high-pass filter and is more sensitive to the activities of superficial motor units of the muscle directly below the measurement site, making it less susceptible to recording crosstalk [47].

2.3. Electromyographical Features in Fatigue Detection

Throughout the literature, many sEMG features have been investigated for use in muscle fatigue detection/analysis. The most widely explored features used in fatigue analysis are those that are calculated in the time or frequency domain. This is because these features best characterize changes in muscle fiber conduction velocity, motor unit recruitment, and time synchronization in the activity of particular motor units (MUs) [5], [48]. The most commonly used features to characterize these parameters would be the Average Rectified Value (ARV), Root-Mean-Square (RMS) in the time domain and the Mean Frequency (MNF) and Median Frequency (MDF) in the frequency domain [49]–[52]. Wavelet features has also been well-studied and successfully detected and/or predicted fatigue [5], [53]–[55]. A variety of other parameters have been used to study muscle fatigue in the form of autoregression analysis, entropy , recurrence quantification analysis, higher-order statistics and composite features [49]. Coherence is another way of detecting fatigue by the correlated activity of simultaneously active MUs, which is considered an important physiological principle that occurs as muscle fatigue progresses [8].

Although coherence has been gaining traction as a means of detecting muscle fatigue, it remains relatively unexplored. To this end, coherence was chosen as the primary feature investigated in the work presented in this thesis. The study also compared the performance of this feature with the ARV, RMS, MNF and MDF features in the time and frequency domain as they are used most often in the detection of muscle fatigue in the literature.

2.3.1. Coherence

As previously discussed, many modifications in both the central and peripheral nervous system occur during a fatiguing contraction. One such mechanism that has been commonly suggested in the literature as of late is the alteration of the degree of synchronization between the firing times of simultaneously active MUs [8]. In detail, a pair of motor neurons within a motor pool receive neural input, one proportion is common synaptic input to the entire motor pool, while another proportion is independent input [56]. This common synaptic input is responsible for correlated firing of the pair of motor neurons, and the strength of this correlation is known as motor unit synchronization (MU synchronization). MU synchronization can be measured using correlation analysis in either the time or frequency domain. When the correlation is quantified in the frequency domain, it is known as coherence. Coherence derived from a pair of EMG signals (EMG-EMG coherence) quantifies the common synaptic input either between muscles (intermuscular coherence) or between parts of the same muscle (intramuscular coherence) [57], [58]. The detected coherence are typically separated into different frequency bands, including delta (1-4 Hz), alpha (8-15 Hz), beta (16-29 Hz) and gamma (30-45 Hz), with coherence in different bands representing different neurological origins [8], [59], [60] . The delta band typically corresponds to “common drive” which is the neural input received by all the MUs in the motor pool that is later translated into individual firing rates [8], [61]. The origin of alpha coherence is

still unclear in the literature, however some studies have suggested a relation to physiological tremor and a central origin[62]–[64]. Both beta and gamma bands reflect information from oscillatory cortical and sub-cortical processes within the cortico-spinal pathway, where these processes are known to correlate to MU synchronization [8], [65].

Several studies have shown that there are changes in intermuscular coherence during a fatiguing contraction. This was most prominent in the beta coherence band, where an increase was seen in synergistic hand muscles during index finger flexion [66], knee extensor muscles [67], antagonistic elbow muscles [68], and three digit grasping [69]. Furthermore, a study was conducted that assessed the differences in fatigue development between the young and elderly which revealed that there was age-specific reductions in beta-band coherence between specific ankle muscles during gait [70]. In contrast to these studies, some have recorded no significant increase in beta band coherence but rather showed increased coherence in other bands such as an increase in alpha band coherence between elbow flexor muscles [71] , and synergetic quadricep muscles [72]. In addition to this, one study reported no changes in alpha or beta band coherence but a decrease in delta coherence within unilateral plantar flexors during a fatiguing task [73].

Although not as many, there are studies that have investigated the relationship between fatigue and intramuscular coherence. Analysis of intramuscular coherence of the first dorsal interosseous muscle reported increases in delta, alpha and beta band coherence following a fatiguing contraction [8], [74]. Investigation of the biceps brachii revealed an increase in alpha band coherence after a isometric contraction of elbow flexors measured using intramuscular electrodes [75]. Another study examined fatigue through continuous dynamic contractions of the biceps brachii and revealed an increase in beta band energy of the intramuscular coherence profile using HD-sEMG electrodes [76]. Current fatigue analysis of intramuscular coherence generally

uses composite MU spike trains derived from either decomposition techniques of sEMG signals or through intramuscular electrodes. Analyzing intramuscular coherence for the detection of fatigue using interference sEMG signals have yet to be explored. Additionally, the use of intramuscular coherence to assess age-associated differences in fatigue generation is not explored either.

2.3.2. Time-Frequency Domain Features

As muscle fatigue progresses, the recorded sEMG signal undergoes changes in its amplitude and spectral content [49], [77], [78]. This is due to the effect of conduction velocity reduction, which acts as a scaling factor for EMGs amplitude and associated power spectrum [79]. The changes in amplitude can be quantified using ARV and RMS, which are commonly used metrics in the literature to quantify fatigue [49]. Both of these metrics are known to increase substantially at the beginning of a contraction, then increase gradually until mechanical failure [80]. The power spectrum of the EMG signal compresses during a fatiguing contraction because of the reduction of conduction velocity and can be measured using both MNF and MDF. Multiple studies revealed that compression of the power spectrum leads to a decreasing trend in both MNF and MDF as fatigue accumulates [49], [52], [80]. Although these features are widely used, there are several limitations that keep them from being global indicators of muscle fatigue. One principle limitation is the fact that a change in conduction velocity is not the only factor in determining changes in sEMG signals [79], [81]. To account for these other factors, different indices are explored to evaluate their ability to detect fatigue.

3. Methods

3.1. Subjects, Systems and Procedures

Seventeen male subjects free from physical impairment were recruited from the University of Waterloo to participate. Subjects were split into two groups according to age; the young group comprised of 10 subjects between the ages of 22 and 30 years old (24.40 ± 2.42 years) and the elderly group had 7 subjects between ages 68 and 75 years old (72.85 ± 2.67 years). The weight and height of every subject was measured as well as their arm length and diameter, the former of which was used for BMI calculations. Max torque was also recorded as the force outputted during

Table 1: Young subject demographics and relevant data.

Subject ID	Age (years)	BMI (Kg/m^2)	Max Torque (N.m)	Arm Length (cm)	Arm Diameter (cm)
1	23	24.82	110.3	28	32
2	22	21.63	89.0	30	28
3	23	24.33	57.0	34	31
5	23	23.08	88.0	33	30
6	23	23.20	66.0	33	28
7	27	23.12	55.0	33	30
10	22	18.81	52.0	34	25
15	30	21.37	44.0	31	27
16	24	22.01	79.0	34	28
17	26	21.10	62.0	30	27

Table 2: Elderly subjects demographics and relevant data.

Subject ID	Age (years)	BMI (Kg/m^2)	Max Torque (N.m)	Arm Length (cm)	Arm Diameter (cm)
4	75	22.63	54.0	33	30
8	72	27.46	89.0	32	32
9	74	20.92	63.0	35	27
11	75	23.67	35.0	32	27
12	68	23.77	39.0	32	26
13	75	22.26	67.0	32	26
14	71	27.74	44.0	31	31

the 100% MVC contractions. The demographics for all subjects in both groups are presented in Table 1 and Table 3.

All recruited subjects were right hand dominant and using the body mass index (BMI), no subject in either the young group (22.34±1.66) or the elderly group (25.55±3.06) was reported as underweight (BMI ≤ 18.5) or obese (BMI ≥ 30). At the time of the study, the participants did not report any abnormal pathologies, myopathy, and musculoskeletal injury within the past 6 months. Informed consent was obtained from each participant before the experiment and procedures were in accordance with the Declaration of Helsinki.

A HD-sEMG electrode system (EMG-USB2+, OT Bioelettronica, Italy), was used to acquire sEMG data in a monopolar montage. The system recorded signals with a sampling rate of 2048 Hz, and a gain of 500. Following skin preparation, an 8x8 grid of electrodes (10mm inter-electrode distance, 4mm electrode diameter) was placed atop the biceps brachii of the dominant right arm (approximately placed such that the grid lied between 20% and 61% of the upper limb length measured from the elbow; Figure 3). The biceps was chosen as it is a large superficial

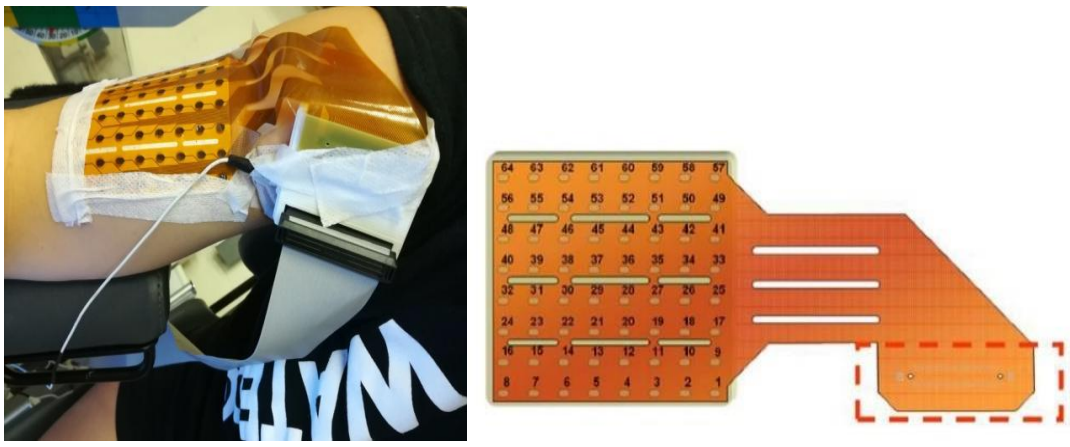

Figure 3: High Density sEMG (HD-sEMG) electrode grid placement on subject and numerical reference of the electrodes.

muscle that is primarily responsible for elbow flexion and has known observable changes in muscle fibers with aging [24].

Subjects used a Dynamometer system (System 4 Pro, Biodex, USA) to generate torque signals during elbow flexion. The system acquired torque signals with a sampling rate of 2048 Hz. Using this system, an isometric contraction is ensured as zero velocity is maintained in all possible range, allowing no significant variations in muscle length or joint angle during contraction. Subjects were seated in the dynamometer with 85° hip flexion from the anatomical position. The dynamometer arm was oriented 30° toward the participant resulting in an elbow angle of 90° prior to elbow flexion. Following calibration, the user was seated with their right elbow resting against a support. The forearm was placed in supination position firmly holding the fixed handle on the dynamometer arm, as seen in Figure 4. Due to the electrodes placed on the arm, it was not possible to immobilize the arm completely.

Figure 4: Dynamometer system during elbow flexion. Arm constraint was removed throughout the protocol to allow for placement of HD-sEMG electrode grid. Taken from [82].

To get used to the experimental setup, subjects first performed test contractions to get a sense of familiarity. Subjects were then instructed to produce maximal voluntary contractions (MVC) by pulling the dynamometer handle towards them at maximal effort and maintaining it for five seconds. This was repeated three times to get an accurate reading of the MVC value. Two-minute breaks were provided between the MVC contractions to minimize the effect of fatigue on the MVC recordings. Following the MVC contractions, subjects rested an additional 2 minutes before continuing the remainder of the protocol. Recording of both sEMG and torque data was started after the rest period and subjects were instructed to perform three quick contractions to allow for realignment between the sEMG and torque data in offline analysis. Subjects were then asked to sustain 20% MVC contraction until a subjectively determined endurance limit, which was defined as "task failure". Subjects were able to see their torque output overlaid with the 20% MVC target on a monitor, allowing them to constantly maintain a force above the 20% MVC torque objective.

3.2. Preprocessing of EMG Data

The EMG data for all subjects in both groups was pre-processed prior to further analysis. The EMG signals recorded were filtered within the EMG-USB2 device using a bandpass filter between 10 and 500Hz. A subject matter expert inspected raw EMG data for quality, identifying channels that either have no signal or excessive noise (<1% of the channels recorded, only found in five subjects). The data of these channels were substituted by the average value of surrounding channels. Subjects that exhibited a signal-to-noise ratio (SNR) under 12dB were excluded from further analysis. The signals recorded were obtained from a monopolar configuration, meaning it is highly susceptible to crosstalk contamination [83]. To mitigate the effects of crosstalk, Bipolar and Laplacian spatial filters were introduced. As the filters may affect the detection of muscle

fatigue, features were calculated with and without these filters applied. This was done to investigate if muscle fatigue detection could be improved depending on the selection of spatial filter. To align the torque and EMG signals together in time, the data obtained from the three brisk contractions prior to the fatiguing contraction was used. An alignment procedure was implemented which calculated the cross-correlation function between the two signals. The position of the peak values of the cross-correlation function was identified, which was then used to realign the EMG and torque signals.

3.2.1. Signal To Noise Ratio (SNR)

For every subject, the signal-to-noise ratio (SNR) was computed to eliminate any participants that had noisy sEMG signals. This metric represents the ratio of the sEMG signal during a contraction over the background noise during the resting periods. The SNR for each recording was calculated using a one second non-overlapping moving window and translating it over the duration of the entire signal. The noise was then determined by taking a one second

*Table 3: Averaged SNR values for each participant. * Indicates subject that was excluded due to SNR lower than threshold value of 12dB*

Young Subjects	SNR (dB)	Elderly Subjects	SNR (dB)
1	24.04	4	24.31
2	23.07	8	14.82
3	*9.34	9	12.06
5	31.74	11	18.02
6	17.19	12	13.97
7	16.19	13	12.33
10	16.83	14	12.67
15	15.36		
16	23.64		
17	29.52		

window of the two-minute rest period in-between MVC contractions at the beginning of the protocol. The SNR values was then averaged over all 64 electrodes on the HD-sEMG grid and

compared to an empirically determined 12dB threshold. One out of the 17 subjects were excluded from further analysis due to being below this threshold. The SNR for every subject is reported in Table 3.

3.2.2. Spatial Filtering

sEMG data was collected using the 64-channel electrode grid and from this grid, spatial filter electrode configurations were constructed. The three spatial filter electrode configurations used in this study is: Monopolar (MP), Bipolar (BP) and Laplacian (LA). MP spatial filter

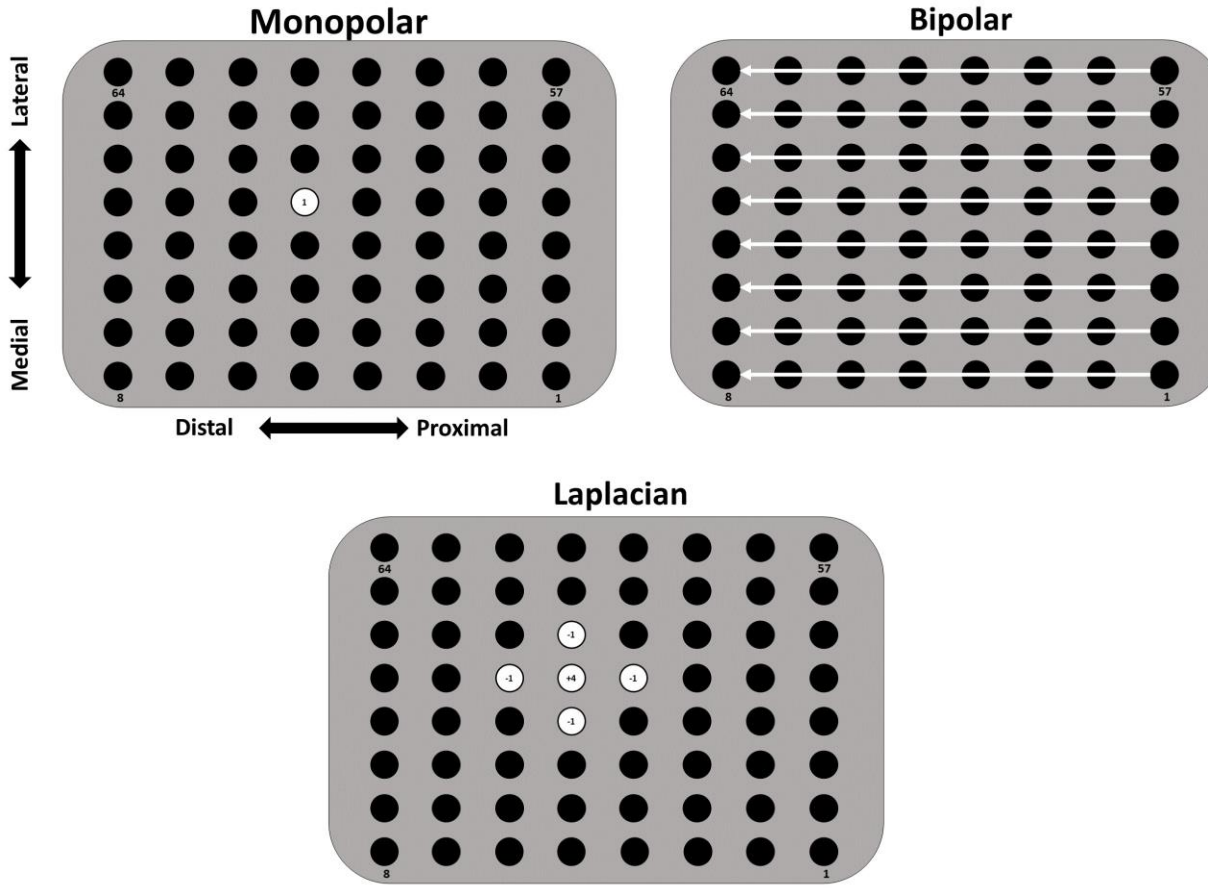

Figure 5: Three different spatial filters derived from 3 different electrode configurations of the HD-sEMG grid: monopolar (MP), bipolar (BP) and Laplacian (LA). All filters are implemented for all available electrodes on the electrode grid.

configuration used the raw EMG signal obtained from each electrode and no further calculation

was used. The BP spatial filter was implemented on the entire grid using the closest-neighbouring electrode pairs in the proximal-distal direction, aligning with the direction of the muscle fiber of the biceps brachii. This resulted in 56 bipolar EMG signals being obtained from the grid (7 longitudinal bipolar recordings except most distal column on grid) by subtracting EMG signals recorded from adjacent electrodes along the muscle fiber direction, as seen in (1)

$$V_i^{BP} = V_i^E - V_{i+1}^E \quad (1)$$

where V_i^E is the sEMG signal recorded from the ith electrode and V_{i+1}^E is the sEMG signal recorded from the signal adjacent to the ith electrode in the distal direction.

The Laplacian spatial filter configuration was also used as it is a spatially high-pass filter and is more sensitive to the activities of the superficial motor units of the muscle directly below the measurement site [47]. As such, it is also less susceptible to surface EMG crosstalk [47]. The Laplacian filter is set up by assigning a fixed weighting factor of '4' to the central electrode, and a factor of '-1' to the nearest neighbouring electrodes, and the output of the filter is the weighted summation of all the channels. This can be computed using equation (2) below.

$$V_i^{LA} = V_i^E - \frac{1}{N}\sum_{j \in S_i} V_j^E \quad (2)$$

where S_i is the set of electrodes surrounding the ith electrode and N is the number of surrounding electrodes [84]. This resulted in 36 Laplacian EMG signals being obtained from the grid as edge electrodes.

3.3. Data Analysis

Features were extracted from the EMG data of both groups to quantify the electrophysiological changes in muscle activity due to fatigue. First, three widely used time and

frequency domain features in the analysis of muscle fatigue were calculated for each filter. These features include the average rectified value (ARV), mean frequency (MNF) and median frequency (MDF). Following this, the pooled intramuscular coherence was calculated for each filter. The coherence was calculated between interference EMG signals on the HD-sEMG grid and were examined in the alpha (11-15 Hz), beta (16-29 Hz) and gamma (30-45 Hz) frequency bands, as explained in the **Coherence Analysis** subsection. This was implemented as coherence allowed for investigation of the correlation between MU discharges in the biceps brachii during a fatiguing contraction [8]. Both conventional fatigue features and coherence was calculated for each filter to compare 1) the ability each filter has to detect fatigue within the young and elderly groups, 2) ability of each filter to detect differences in generation of muscle fatigue between both age groups, and 3) fatigue detection ability between mean coherence values and previously established EMG fatigue features. Following this, the correlation of mean coherence in each frequency band and the variation of torque during the fatiguing contraction was calculated. This was done to assess if there were any age-related differences between the increase in force fluctuations, which is typically associated with muscle fatigue(as seen in [85]) and the various neural mechanisms that are reflected by intramuscular coherence and associated frequency bands.

3.3.1. Torque Analysis

Torque measures were calculated as it allows for the investigation of muscle performance during a fatiguing contraction. Specifically, the variability of torque production was evaluated as there is a considerable amount of evidence reported in the literature that the fluctuations of torque increase with muscle fatigue both during and after a sustained contraction [85]–[87]. Interestingly, although the elderly have been found to be less fatigable than the young, studies have revealed that older adults have a diminished ability to produce consistent torque when compared to young adults

[88], [89]. This is likely due to age related changes in the muscles and/or nervous system such as Sarcopenia [89], [90] and/or changes in inputs to the motoneuron pool [91], [92]. However, these findings suggest that while the elderly have more variability in torque initially, such variability increases in a lesser extent throughout a fatiguing contraction when compared to the young. This reveals potential differences in the physiology behind torque production during a sustained contraction between both groups. As such, the coefficient of variation (CoV) was calculated for each participant in both groups to quantify the fluctuations of torque throughout the fatiguing contraction. This was performed by segmenting the acquired torque signal for each subject into overlapping 25-second segments. The torque signal was recorded with a sampling rate of 2048 Hz, the same as the EMG signals, to avoid synchronization issue. For the first epoch, the CoV of the first 25 seconds of the torque signal was calculated. The epoch was then shifted 1 second forward in time (2048 samples) and then CoV was calculated for the following 25 seconds, which caused an overlap of 96%. This shifting in time was iterated from the first epoch, Epoch 1 through Epoch 'n-25', where n is the length of the torque signal in seconds. This segmentation process is shown below in Figure 6.

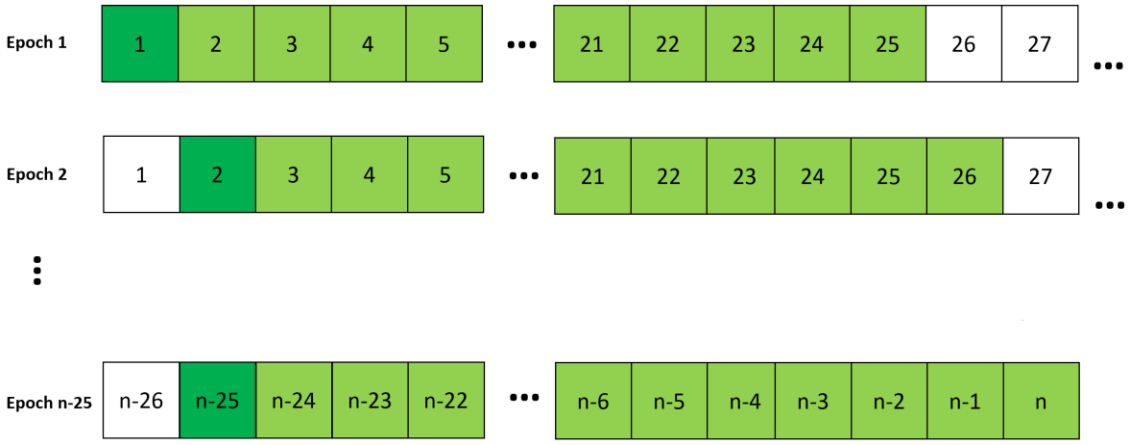

Figure 6: Overview of the torque segmentation method. Each square corresponded with one second in the torque signal. Every 1 second window represents 2048 torque samples. The first second (dark green) corresponding with the epoch number and the rest of the epoch (light green) was used to calculate the CoV.

3.3.2. Time and Frequency Feature Analysis

Three of the most widely used features in the time and frequency domain for analysing muscular fatigue are extracted from the HD-sEMG signal for every filter. In the time domain, the average rectified value (ARV) and root-mean-square (RMS) were calculated and used to characterize the amplitude of the EMG signals. Both ARV and RMS is used to provide insight into the activity of the muscle under fatiguing conditions, and is calculated using the following discrete equation [5], [52]:

$$ARV = \frac{1}{N_{tot}} \sum_{i=1}^{N_{tot}} |x_i| \tag{3}$$

$$RMS = \sqrt{\frac{1}{N_{tot}} \sum_{i=1}^{N_{tot}} x_i^2} \tag{4}$$

where N_{tot} is the number of samples in the selected time window, and x_i is the i^{th} sample of the analyzed sEMG signal. Both the mean (MNF) and median frequency (MDF) features were

calculated in the frequency domain. These parameters were extracted from the power spectral density (PSD) of the EMG signal, estimated by the Welch method. Both features are used to represent the spectral component of the EMG signal, which provides information about the muscle fibres conduction velocity during fatiguing contractions. To calculate the spectral features, the entire EMG signal was split into smaller time-windows. Each window is further split into 5 sub-windows where the periodogram has been estimated for each sub-window and then averaged over the 5 sub-windows. The following discrete expressions were used to calculate both MNF and MDF.

$$MNF = \frac{\sum_{k=1}^{F_{tot}} f_k S_k}{\sum_{k=1}^{F_{tot}} S_k} \quad (5)$$

$$\sum_{k=1}^{MDF} S_k = \sum_{k=MDF}^{F_{tot}} S_k \quad (6)$$

where F_{Tot} is the total frequency bins and S_k is the magnitude of the power spectrum at the kth bin.

3.3.3. Coherence Analysis

Coherence analysis was utilized to assess the linear correlation between the spectral components of different motor units within the biceps brachii. Coherence was studied throughout the bicep brachii by pooling the coherence calculated from the electrodes furthest apart in the medial-lateral direction on the HD-sEMG grid. This was done to minimize the effect crosstalk may have on the coherence spectra. Prior to coherence analysis, no additional filters were applied to avoid the effect filtering may have on coherence. Rectification is often recommended for EMG

signals prior to coherence analysis because of its ability to facilitate the detection of oscillatory inputs by increasing the spectral power associated with these inputs [93]. However, rectification itself is a nonlinear process that effects the frequency components of the original signal [94], [95]. As stated in [95], rectification should be implemented if there is a low amount of amplitude cancellation, which is associated with low contraction levels. Although a low contraction level (20% MVC) is used, as it is a fatiguing contraction the amplitude cancellation increases due to the recruitment of additional MUs, increased MU potential duration and change in amplitude [96]. Consequently, EMG signals were not rectified prior to coherence calculations to limit the adverse effects associated with the rectification process. All coherence analyses reported in this study was implemented in the Neurospec toolbox for MATLAB (www.neurospec.org, Version 2.0, 2008 ,see [97] for theoretical framework). Coherence analysis was based on the spectral estimates of the EMG signals for each electrode in the electrode pair. Non-overlapping windows of one second (segment length of 2048 samples) were used resulting in spectral plots having a resolution of 1 Hz per bin. The magnitude squared coherence, $|C_{xy}(f)|^2$, between two EMG signals recorded from two different electrodes, x(t) and y(t), for a frequency f was calculated as

$$|C_{xy}(f)|^2 = \frac{|S_{xy}(f)|^2}{S_{xx} \cdot S_{yy}} \qquad (7)$$

where $S_{xx}(f)$ and $S_{yy}(f)$ are the auto spectra of each signal and $S_{xy}(f)$ is the cross spectra. Coherence provides a measure of linear association of the two signals at each frequency on a scale of 0 to 1, where 0 shows no correlation and 1 means the two signals are identical. In other words, coherence estimates show how much of the EMG signal of one surface electrode can predict the activity in another EMG signal from a different electrode. Using this, coherence can help detect

fatigue by quantifying the frequency content of common presynaptic input to MUs [16], [98]. Significance thresholds of coherence measure were determined through

$$CI = 1 - \alpha^{\frac{1}{L-1}} \tag{8}$$

where CI stands for confidence interval, α is the confidence level, which was set to be 0.05 to correspond with a 95% confidence limit and L is the number of segments used in the coherence calculation [97] .

The spatial information that the HD-sEMG provides was leveraged to provide a more holistic view of the muscle. To do this, the correlation structure of the multiple electrode pairs was combined to form an estimate of coherence. This is known as pooled coherence which provides a single value which represents this correlation structure at the population level across several data sets [99] . Pooled coherence is similar to individual coherence as it is also measures linear association on a 0 to 1 scale but differs in that any inferences relate to the population (pairs of electrodes) as a whole rather than an individua l pair of electrodes [100]. The pooled coherence, $C_{Pool}(f)$, at frequency f is defined as

$$C_{Pool}(f) = \left| \frac{\sum_{i=1}^{k} L_i C_{xy}^{i}(f)}{\sum_{i=1}^{k} L_i} \right|^2 \tag{9}$$

where $C_{xy}^{i}(f)$ is the individual coherency (not to be confused with coherence $\left|C_{xy}(f)\right|^2$) calculated from L_i segments of EMG data for each individual record (in the context of the present study, this equates to electrode pair) i, calculated within a population consisting of a total number of records (total electrode pairs) k.

To compare the coherence more accurately across participants in different age groups and filter types, the raw pooled coherence estimates was normalized using a Fischer z-transformation [101], [102]. This normalization transforms the data to normal distribution with zero mean and unit variance. The transformation was defined as

$$Z_{xy}(f) = \sqrt{2L}\,\text{atan}h\left(\sqrt{C_{pool}}\right) \quad (10)$$

where $Z_{xy}(f)$ is the resultant z-score after z-transformation and L is the number of segments used in the estimation of the entire coherence plot. Fisher z-transformation is typically used in coherence analysis as it stabilizes the variance of the coherence estimates allowing for more accurate statistical results [69].

The z-score of the pooled coherence was calculated for every subject within both groups separately to determine 1) which spatial filter is the most capable at detecting fatigue related differences in intermuscular coherence, 2) if there are age-related differences in the coherence profiles during fatigue, and 3) identify if there is a correlation between CoV of torque and coherence in both groups. The mean coherence was analyzed in the alpha (11-15 Hz), beta (16-29 Hz) and gamma (30- 45 Hz) frequency bands for both pre- and post-fatigue conditions. The length of each fatigue condition changed depending on the analysis, with analysis 1) and 2) utilizing the first and last 25 seconds of the contraction for the pre- and post-fatigue conditions respectively. The first 25 seconds was used as it is representative of the muscle with minimal fatigue. The 25 seconds prior to task failure was analysed as it can provide insight into the physiological processes underlying the generation of muscle fatigue [103]. Usage of a smaller time-window of 25 seconds is leveraged through the usage of the spatial information from the multiple electrodes pooled. This allowed for conclusions to be made about the fatigue state of the muscle from time windows that

are considerably shorter when compared to other similar studies [68], [69]. Analysis 3) used the first and last 25% of the fatiguing contraction as the considerably longer length allowed for better correlation estimates between the CoV of torque and mean coherence.

3.4. Statistical Analysis

Statistical analysis was first performed on the mean ARV, RMS, MDF and MNF parameters as well as the z-score mean coherence in the alpha, beta, and gamma bands in both the pre- and post-fatigue states. To compare the effect each spatial filter had on time-frequency parameters, a linear regression was performed to assess the change throughout the fatiguing contraction. In addition, Mann-Whitney U tests were utilized to investigate 1) if there was a significant difference between fatigue states within each of the young and elderly groups and 2) if there was a difference in fatigue generation between both young and elderly groups. This analysis was repeated for each of the MP, BP, and LA spatial filters. Next, the CoV of the mean coherence calculated in every frequency band was calculated for each filter type. These results were compared with one another using Mann-Whitney U tests to examine the consistency of coherence measured throughout the contraction. The effect force steadiness had on mean z-score coherence was investigated using Spearman's rank correlation for each frequency band. For all analyses, the level of significance was set to 0.05.

4. Results

The data from one subject had been removed from the analysis due to predominately poor SNR. An additional two subjects were removed from the study because they voluntarily stopped sustaining the contraction before their muscle fatigued as indicated by positive trends in ARV values. As a result, 8 and 5 subjects remained in the young and elderly group, respectively. An example of the raw sEMG and torque signals taken from a representative subject throughout the fatiguing contraction is shown in Figure 7.

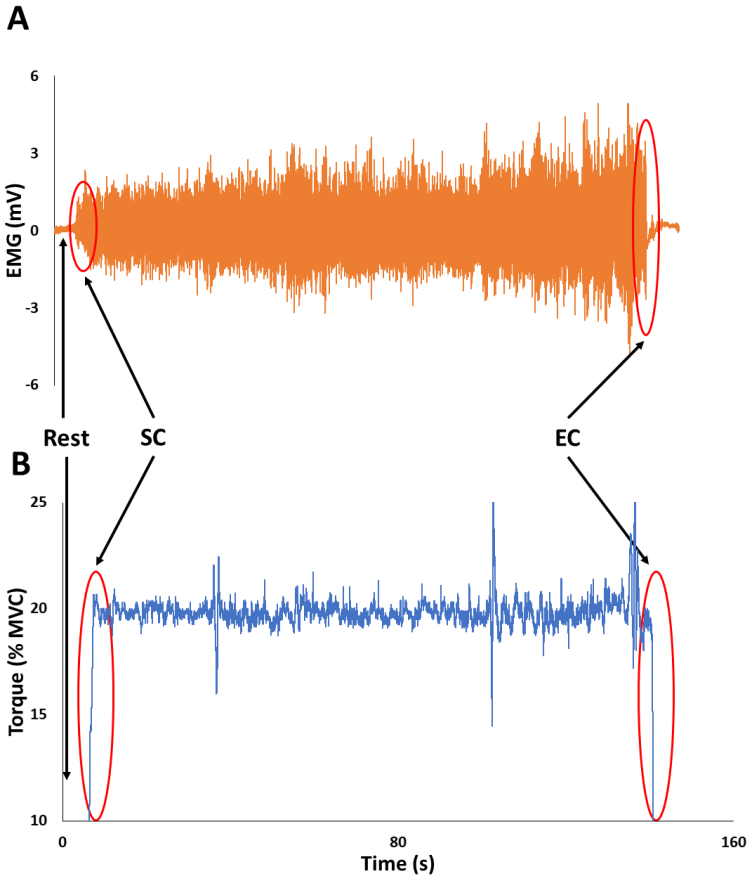

Figure 7: A) EMG signals and B) Torque signals taken during the fatiguing contraction for a representative subject. Rest is when the subject is at rest prior to the contraction starting. The start of the contraction (SC) represents when the subject starts the fatiguing contraction and end of the contraction (EC) represents when the subject reaches task failure and is no longer able to sustain the contraction.

4.1. Effect of Spatial Filter on Time Frequency Feature Extraction

For every spatial filter, the ARV, RMS, MNF, and MDF time and frequency domain parameters were calculated, and tracked over the fatiguing contraction, as seen on a representative subjected in Figure 8. It was observed that there was an increase in both ARV and RMS during the fatiguing contraction, while the MNF and MDF spectral parameters decreased, which is in agreement with what has been reported in the literature [5], [103], [104] .

For each spatial filter, a linear regression was computed for every feature to assess if filter type influenced detection of fatigue related differences between the young and elderly. The

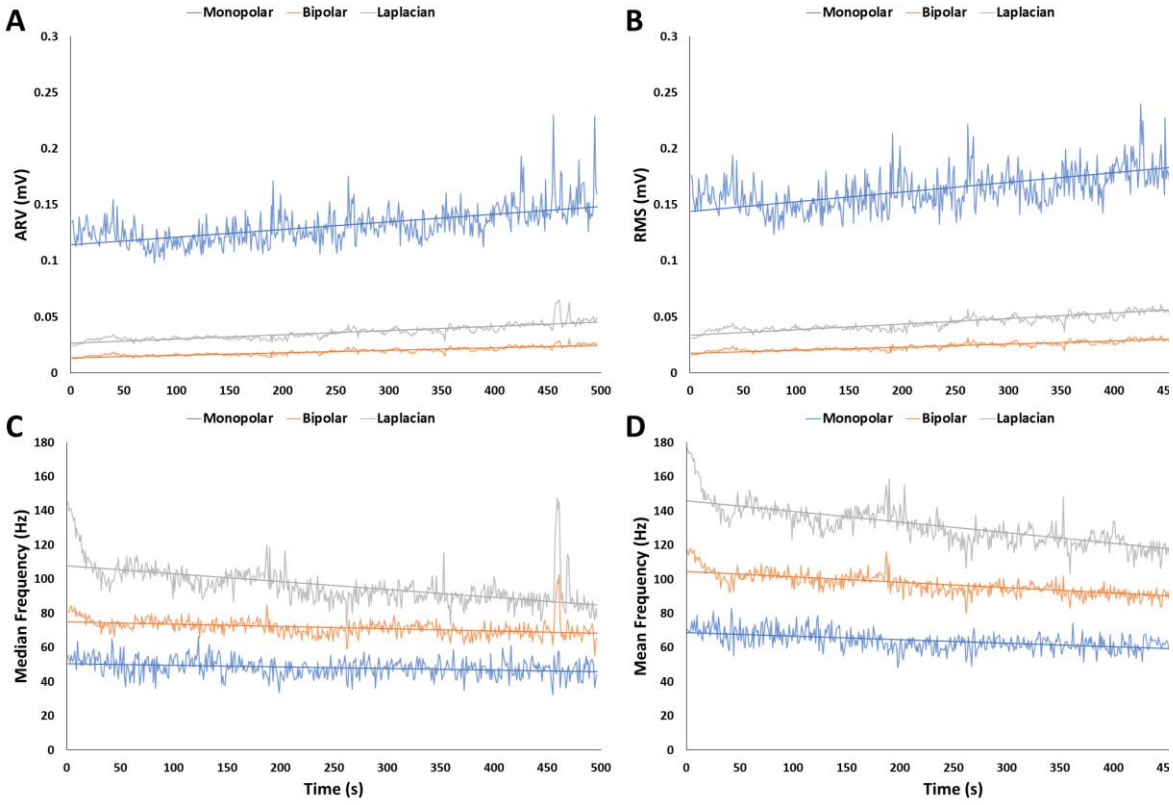

Figure 8: Changes in mean A) ARV, B) RMS, C) MDF, and D) MNF throughout the fatiguing contraction of a representative subject. Each feature was calculated for each of the MP, BP and LA spatial filters. Regression lines were depicted with solid lines along the trace of each feature.

resulting slopes of this analysis are reported in Table 4 for the young population and Table 5 for the elderly population. As the contraction approached task failure, time domain features (ARV, RMS) increased the most rapidly using MP for both groups. MP was also the most sensitive to fatigue related decline in frequency domain features (MDF, MNF) in the young group. However, frequency domain features calculated in the elderly recorded the greatest decline using LA. Although features calculated under the different filters followed similar trends, none were able to distinguish differences in fatigue development between the young and elderly. Mann-Whitney U tests reported non-significant differences between both groups in each of the ARV (MP: p= 0.222; BP: p= 0.093; LA: p=0.127) , RMS (MP: p= 0.1709; BP: p= 0.093; LA: p=0.127), MDF (MP: p= 0.284; BP: p= 0.622; LA: p=0.435), MNF (MP: p= 0.065; BP: p= 0.354; LA: p=0.435) features.

Table 4: Slope values (derived from linear regression of each time-frequency feature (ARV, RMS, MDF, MNF) for every participant in the young population. The slope values for every feature are reported for each of the MP, BP, and LA spatial filter configurations.

	MP				**BP**				**LA**			
Subject #	ARV (μV/s)	RMS (μV/s)	MDF (Hz/s)	MNF (Hz/s)	ARV (μV/s)	RMS (μV/s)	MDF (Hz/s)	MNF (Hz/s)	ARV (μV/s)	RMS (μV/s)	MDF (Hz/s)	MNF (Hz/s)
1	2.719	3.371	-0.197	-0.193	0.712	0.995	-0.077	-0.070	1.079	1.637	-0.028	-0.040
2	0.240	0.286	-0.052	-0.046	0.101	0.140	-0.004	-0.021	0.195	0.294	-0.013	-0.026
3	0.190	0.239	-0.033	-0.036	0.043	0.058	-0.016	-0.021	0.070	0.098	-0.028	-0.035
4	0.068	0.086	-0.010	-0.020	0.021	0.027	-0.012	-0.032	0.038	0.049	-0.045	-0.062
5	0.013	0.016	-0.009	-0.010	0.025	0.033	-0.009	-0.004	0.055	0.070	-0.035	-0.044
6	0.041	0.054	-0.003	-0.017	0.003	0.002	-0.048	-0.063	0.038	0.036	-0.073	-0.079
7	0.137	0.173	-0.009	-0.039	0.037	0.052	-0.010	-0.024	0.044	0.065	-0.024	-0.043
8	0.164	0.198	-0.032	-0.035	0.062	0.079	-0.017	-0.021	0.132	0.171	-0.025	-0.046
Average	**0.447**	**0.552**	**-0.043**	**-0.050**	**0.125**	**0.173**	**-0.022**	**-0.031**	**0.206**	**0.302**	**-0.034**	**-0.047**

Table 5: Slope values (derived from linear regression of each time-frequency feature (ARV, RMS, MDF, MNF) for every participant in the elderly population. The slope values for every feature are reported for each of the MP, BP, and LA spatial filter configurations.

	MP				**BP**				**LA**			
Subject #	ARV (μV/s)	RMS (μV/s)	MDF (Hz/s)	MNF (Hz/s)	ARV (μV/s)	RMS (μV/s)	MDF (Hz/s)	MNF (Hz/s)	ARV (μV/s)	RMS (μV/s)	MDF (Hz/s)	MNF (Hz/s)
1	0.101	0.126	-0.003	-0.016	0.022	0.028	-0.054	-0.036	0.010	0.017	-0.083	-0.094
2	0.124	0.155	-0.012	-0.021	0.021	0.026	-0.031	-0.024	0.036	0.046	-0.046	-0.045
3	0.023	0.028	-0.014	-0.018	0.003	0.003	-0.011	-0.013	0.008	0.010	-0.009	-0.001
4	0.086	0.106	0.0003	-0.002	0.057	0.075	-0.009	-0.008	0.107	0.147	-0.003	-0.003
5	0.032	0.041	-0.016	-0.016	0.002	0.004	0.007	0.004	0.004	0.006	0.011	0.007
Average	**0.073**	**0.091**	**-0.009**	**-0.015**	**0.021**	**0.027**	**-0.019**	**-0.015**	**0.033**	**0.045**	**-0.026**	**-0.027**

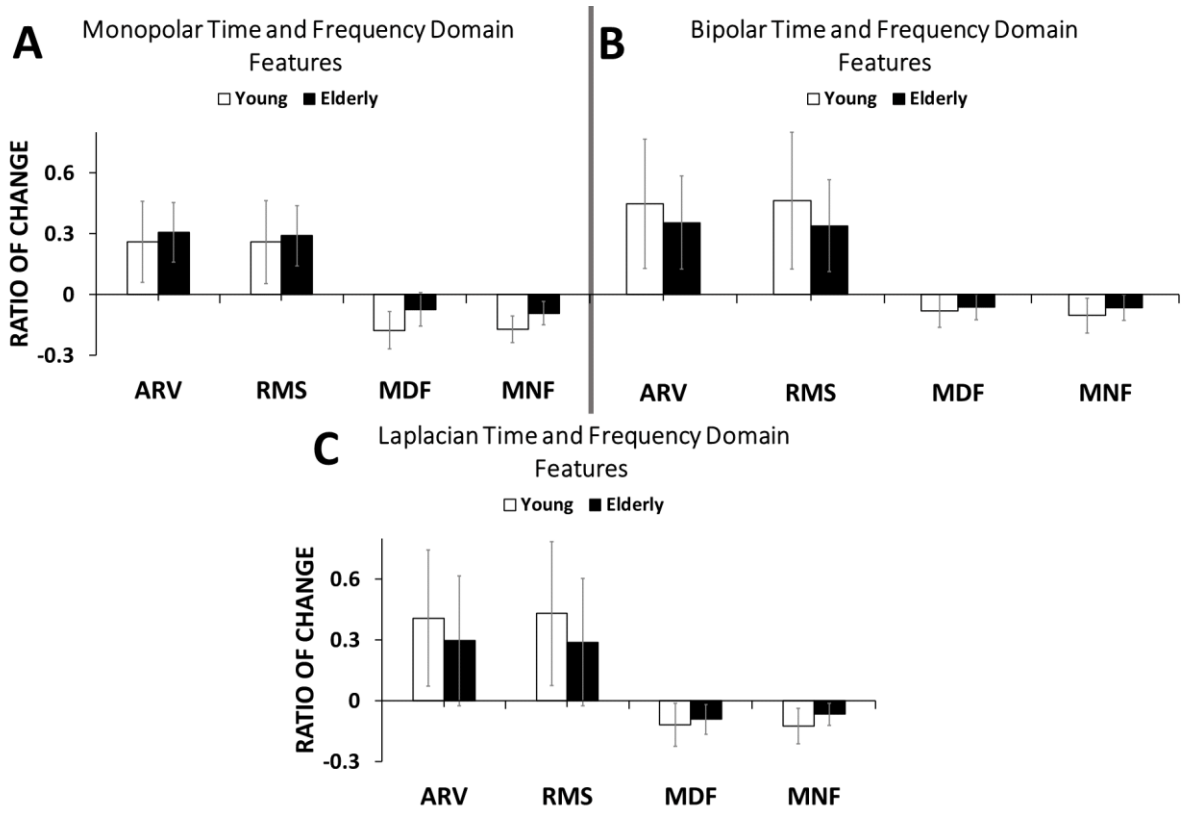

Figure 9: The ratio of change of conventional sEMG features., ARV, MNF, MDF pre- and post-fatigue, for young (white) and elderly (black) subjects. The ratio of change is used to represent the ratio of the respective metrics obtained in the first 25 seconds of the contraction and the last 25 seconds, just prior to task failure.

In addition, a 'ratio of change'' was formed between the feature values calculated within the first 25 seconds of the contraction and the final 25 seconds prior to task failure to highlight changes when fatigue is at its maximum. This was calculated for the features calculated under every spatial filter, shown in Figure 9

It was observed that both ARV and RMS in the young group exhibited larger average change throughout the fatiguing contraction when compared to elderly. However, these features calculated using MP revealed that the young group (ARV: 26.02%, RMS: 25.89%) changed less throughout the contraction than the elderly (ARV: 30.69%, RMS: 29.02%). The BP spatial filter showed the largest ratio of change in ARV and RMS between the three filters. The ARV increased

43% and RMS increased 44.37% for the young population, whereas the elderly increased 34% and 32.58% respectively, throughout the fatiguing contraction.

Irrespective of filter type, the two frequency domain indices (MDF and MNF) showed larger changes in the young population. In the case of MDF, the LA filter observed the largest change as the muscle fatigued with a decrease of 9.29%, whereas both MP and BP decreased 6.04% and 7.34% respectively. MP had the biggest difference in MNF as it decreased 9.33% when compared to BP and LA which decreased 6.37% and 6.84% respectively.

Although the trends are observable and the ratio of change seemed to be non-zero, regardless of the spatial filters and features used, no statistically significant differences existed between the young and elderly: ARV (MP: $p=0.222$; BP: $p=0.833$; LA:0.435), RMS (MP: $p=0.2844$; BP: $p=0.7242$; LA:0.3543), MDF (MP: $p=0.093$; BP: $p=0.833$; LA:0.833), MNF (MP: $p=0.127$; BP: $p=0.724$; LA:0.222).

4.2.Effect of Spatial Filter on Coherence

The effect each spatial filter had on the pooled intramuscular coherence values on 2 representative subjects (1 young subject and 1 elderly subject) are shown below in Figure 10. Pre- and post-fatigue coherence plots is shown to highlight the effect each spatial filter had on the detection of fatigue.

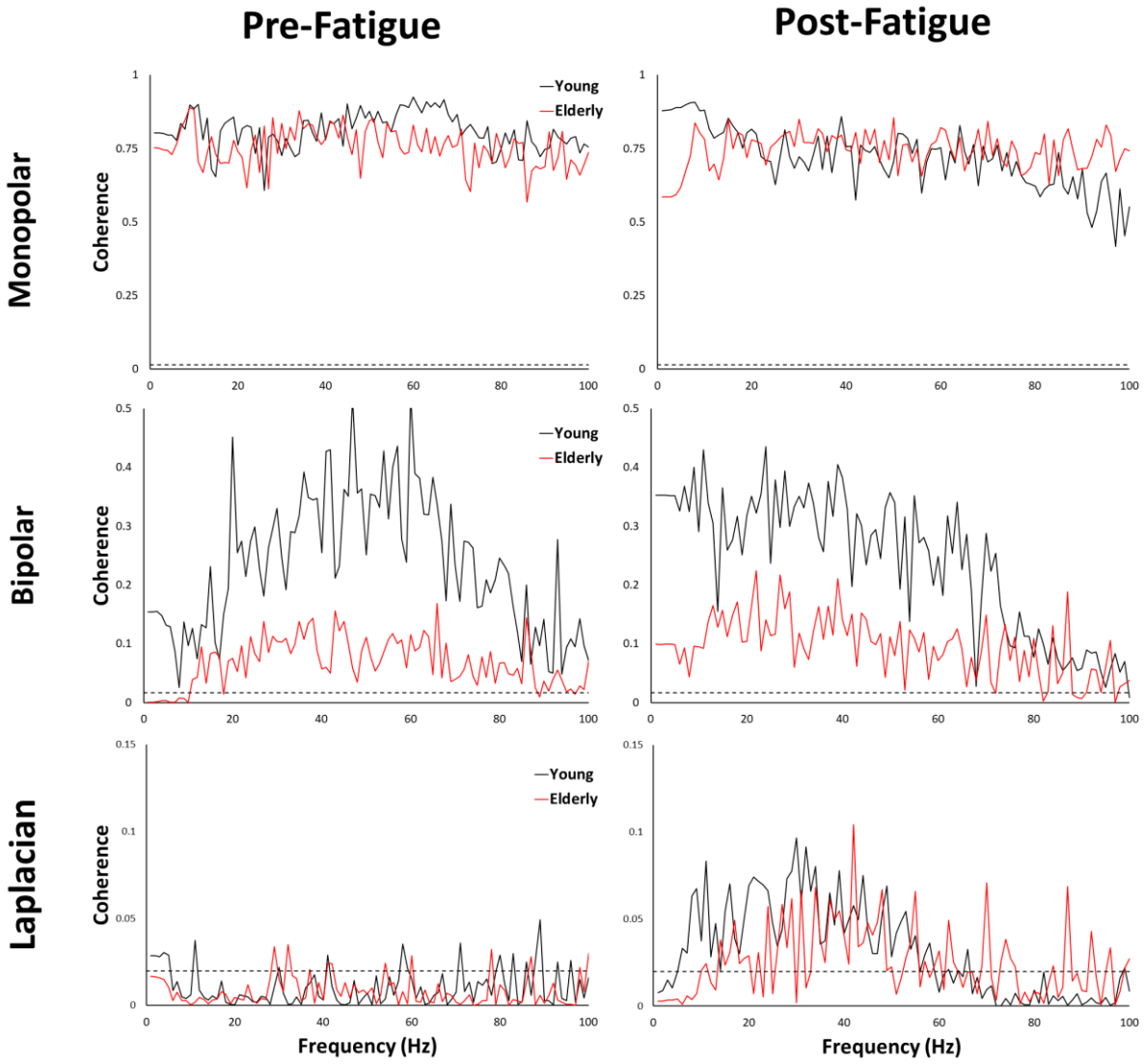

Figure 10: Coherence plots from one representative subject from the young population (Black) and a subject from the elderly population (Red). Coherence is shown for both Pre- and Post-fatigue conditions, and for each condition the resultant coherence plots from the Monopolar, Bipolar and Laplacian spatial filters are given. The horizontal dotted lines represent the 95% confidence limit of coherence.

For both the young and elderly representative subject, LA filtering appeared to be the most sensitive to fatigue related changes. This can be observed in its coherence plot which showed a substantial increase in its coherence values after fatigue, particularly in the 11-55Hz range. The coherence values in this range transitioned from being mostly below significance level (calculated to be 0.0199) at the start of the task to being well above significance prior to task failure. Revealing possible fatigue related changes in the alpha (11-15Hz), beta (16-29Hz) and low gamma (30-45Hz) frequency bands of the coherence profile. Both MP and BP filters did not capture any significant changes in coherence pre- and post-fatigue in either participant. It was observed that the MP and BP filters resulted in coherence values far above significance levels, with the former showing no coherence below the significance level. Analysis of the different frequency bands of both young and elderly groups using mean coherence distributions for each spatial filter are presented in Figure 11.

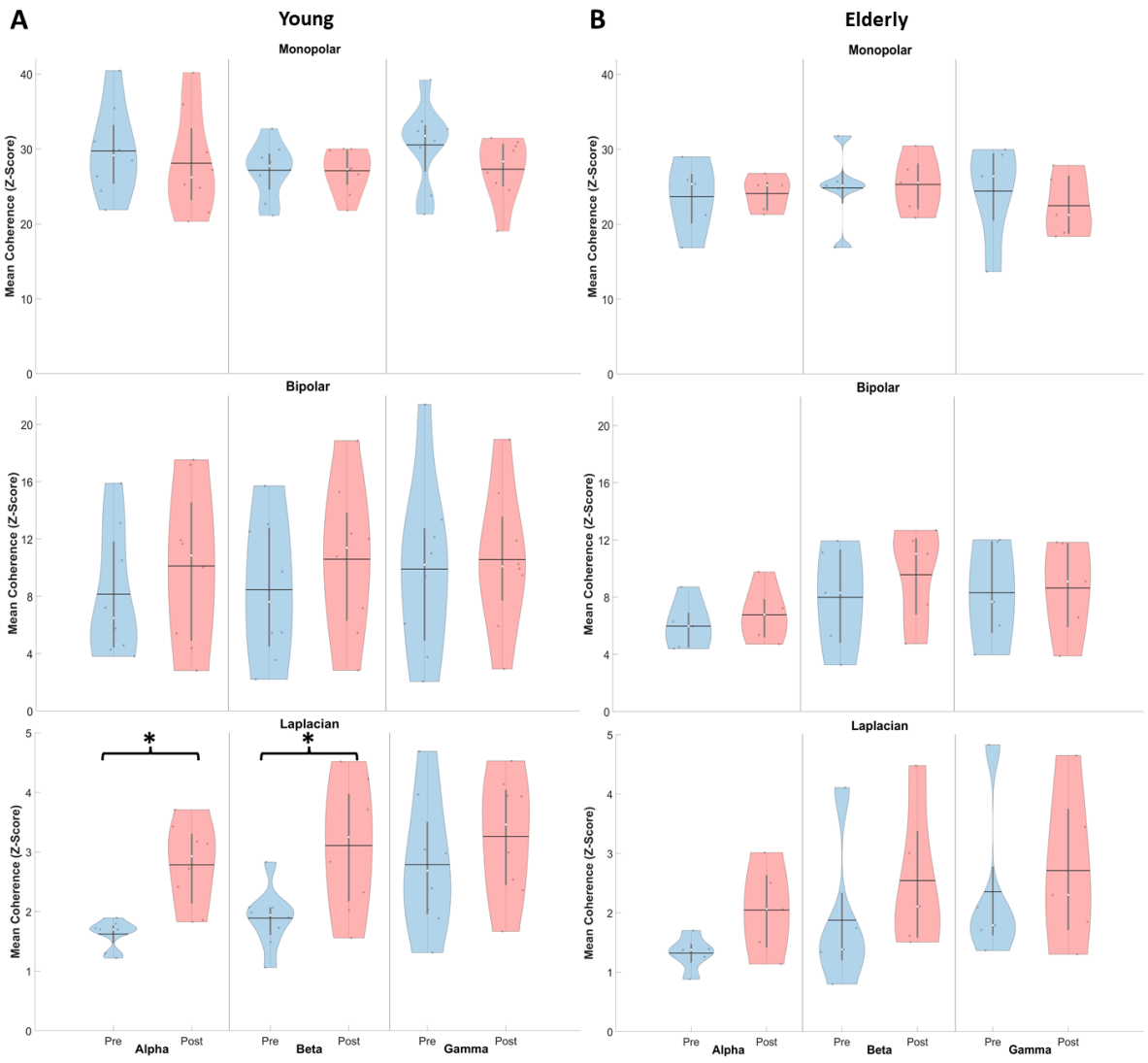

*Figure 11: Violin plots showing the distribution of mean coherence values across participants from both (A) young and (B) elderly groups. Distributions are shown for each of the Monopolar (first row), Bipolar (second row), and Laplacian (third row) spatial filters, and for each filter the pre- and post-fatigue distributions are given for the alpha, beta, and gamma frequency bands. * Indicates significant differences ($p<0.05$) between both pre- and post fatigue conditions.*

Analysis of both groups revealed a similar trend to that of the singular subject, with MP having the highest mean coherence values, followed by BP and LA. Statistical analysis revealed no significant differences in mean coherence during pre- or post-fatigue conditions between the young and elderly groups for any of the MP, BP, and LA filters, seen in Table 6. Suggesting that the spatial filters are not sensitive to age-related changes in mean coherence values, either pre- or post-fatigue.

Table 6: Mann-Whitney U test results comparing pre- and post fatigue conditions of both young and elderly age groups. Where p-values are calculated for each of the alpha, beta, and gamma frequency bands.

	Young	Elderly	p-value		
			Alpha	Beta	Gamma
Monopolar	Pre-Fatigue	Pre-Fatigue	0.0932	0.3543	0.0653
	Post-Fatigue	Post-Fatigue	0.3543	0.5237	0.0932
Bipolar	Pre-Fatigue	Pre-Fatigue	0.7242	0.7242	0.7242
	Post-Fatigue	Post-Fatigue	0.3543	0.8329	0.5237
Laplacian	Pre-Fatigue	Pre-Fatigue	0.1709	0.3543	0.4351
	Post-Fatigue	Post-Fatigue	0.1274	0.4531	0.4351

When comparing pre- and post-fatigue conditions, both LA and BP filters recorded an increase in mean coherence whereas MP generally recorded a decrease in young and elderly subjects. However, only the LA filter recorded significant differences in coherence between both fatigue conditions within the young group. Specifically, LA was sensitive to changes in coherence in the alpha ($p=0.0006$), and beta ($p=0.0207$) frequency bands but not gamma ($p=0.5054$). Coherence values calculated within the elderly group using the same LA filter resulted in nonsignificant changes between fatigue conditions in the alpha ($p=0.1508$), beta ($p=0.2222$), and gamma($p=0.6905$) bands.

4.3. Variability in Torque and Coherence

For both groups, the correlation between mean coherence in all frequency bands and windows (length of time) is presented in Figure 12. This correlation was calculated for both the initial 25% (I25) of the contraction and the final 25% (F25) of the contraction prior to task failure. When comparing I25 and F25 of both groups, the young group consistently exhibited higher mean coherence in all frequency bands. Interestingly, significant positive correlations between time and

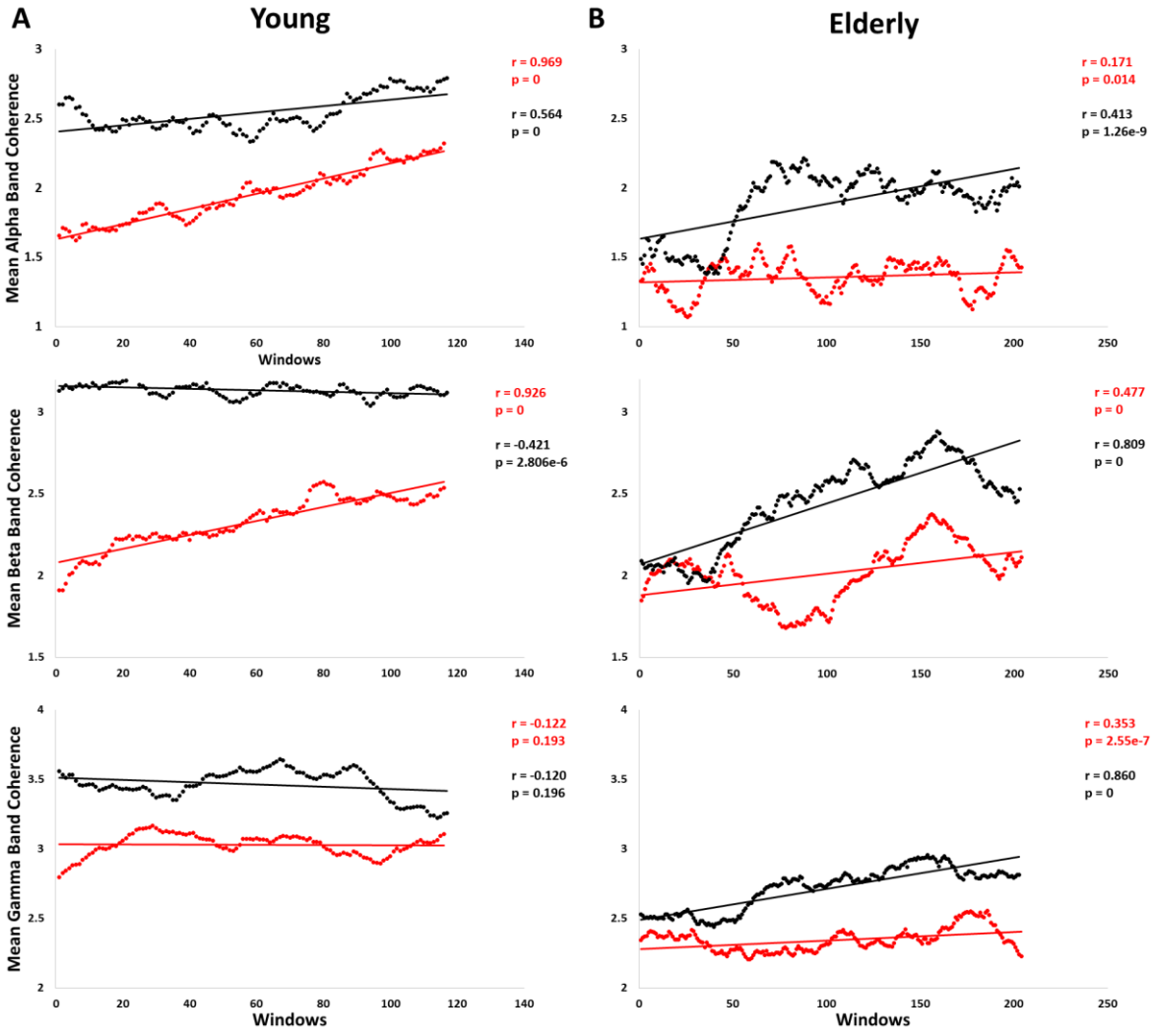

Figure 12: Scatter plot of the windows (time) and i) mean Alpha, ii) mean Beta, and iii) mean Gamma coherence are shown for A) Young and B) Elderly participants. Associated r and p-values are calculated using Spearman's rank correlation. Correlations calculated for the first 25% of the contraction (red) and the last 25% of the contraction (black) prior to task failure.

each of the mean alpha (I25: r=0.171, p=0.01; F25: r=0.413, p=1.26e-9), mean beta (I25: r=0.477, p=0; F25: r=0.809, p=0) and mean gamma (I25: r=0.353, p=2.55e-7; F25: r=0.860, p=0) coherence bands is observed for the elderly group. The young group showed similar behaviour in the alpha coherence band where it displayed significant positive correlation (I25: r=0.969, p=0; F25: r=0.564, p=0). This was consistent in mean beta coherence calculated from the initial 25% of the contraction, which showed significant positive correlation (r=0.926, p=0). However, mean beta coherence calculated from the final 25% of the contraction showed significant negative correlation (r=-0.421, p=2.61e-6). Correlations calculated using mean gamma coherence in the young group displayed nonsignificant negative correlation (I25: r=-0.122, p=0.193; F25: r=-0.120, p=0.196).

The elderly group also showcased significant positive correlation between CoV of torque and mean alpha (I25: r=-0.012, p=0.099; F25: r=0.511, p=0), beta (I25: r=0.448, p=2.33e-11; F25: r=0.643, p=0), and gamma coherence (I25: r=0.264, p=0.0001; F25: r=0.636, p=0) as seen in Figure 13.Similarly, the young group also has significant positive correlation between mean alpha coherence and CoV of torque (I25: r=-0.090, p=0.337; F25: r=0.387, p=1.87e-5) at the final 25% of the contraction. Interestingly, the correlation of CoV of torque and mean beta (I25: r=-0.182, p=0.051; F25: r=-0.297, p=0.001) and gamma (I25: r=-0.069, p=0.461; F25: r=-0.245, p=0.007) coherence in the young exhibited the opposite behaviour to the elderly, with both showing significant negative correlation at the end of the contraction.

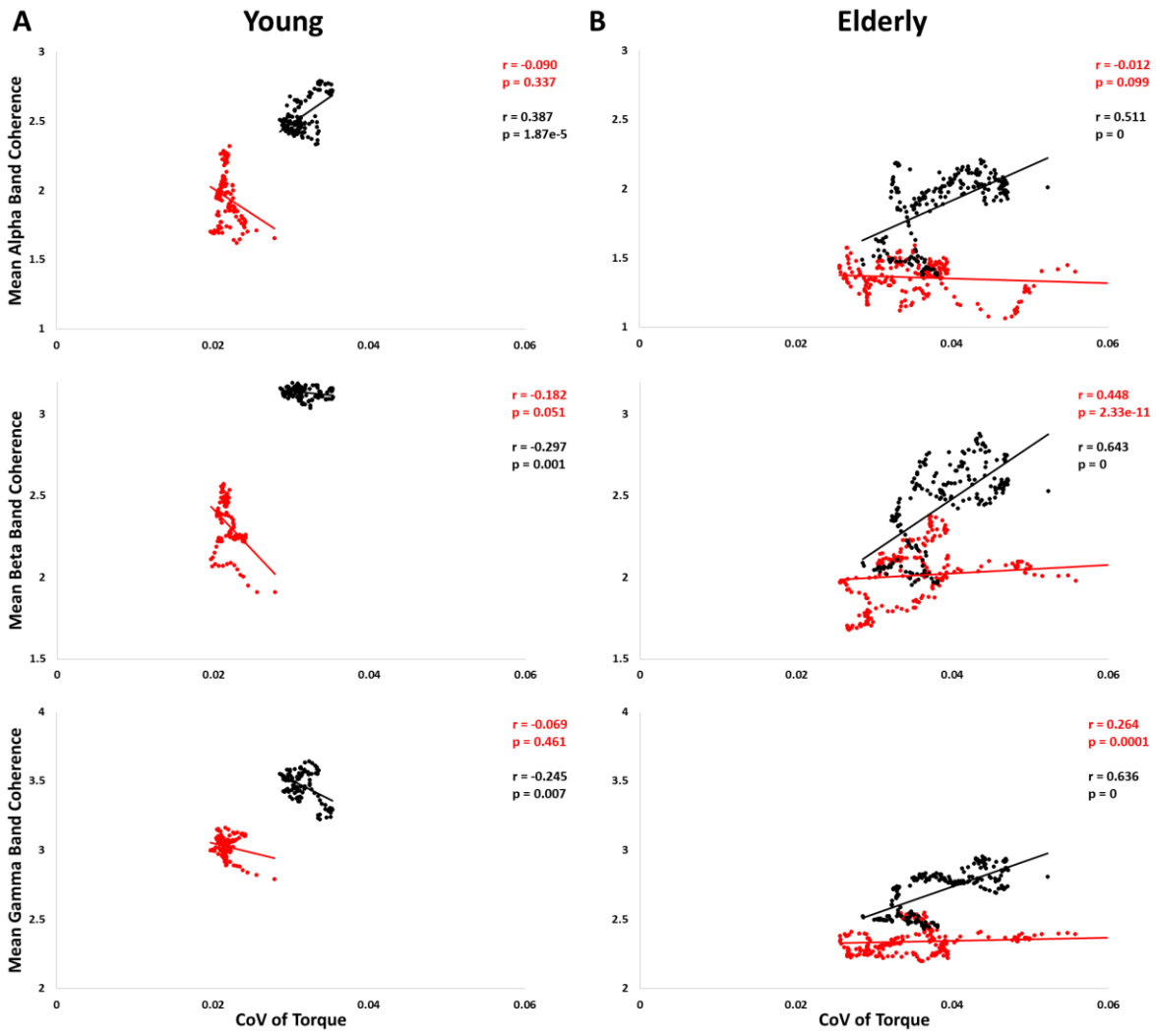

Figure 13: Scatter plot of average CoV of torque and i) mean Alpha, ii) mean Beta, and iii) mean Gamma coherence are shown for A) Young and B) Elderly participants. Associated r and p-values are calculated using Spearman's rank correlation. Correlations calculated for the first 25% of the contraction (red) and the last 25% of the contraction (black) prior to task failure.

As expected, the elderly group typically showcased higher CoV of torque when compared to the young group throughout the contraction. Interestingly, although both groups did exhibit a rise in CoV of torque, the young group had a much steadier rise whereas the elderly seemed to oscillate. Correlation between CoV of torque and windows, as shown in Figure 14, revealed that both young (r=0.479, p=6.48e-8) and elderly (r=0.565, p=0) groups showed significant positive correlation at the final 25% of the contraction. The elderly group displayed significant negative correlation (r=-0.404, p=1.96e-9) between CoV of torque and windows at the initial 25% of the

contraction, while the young group also showed a negative correlation (r=-0.112, p=0.231), it was not statistically significant.

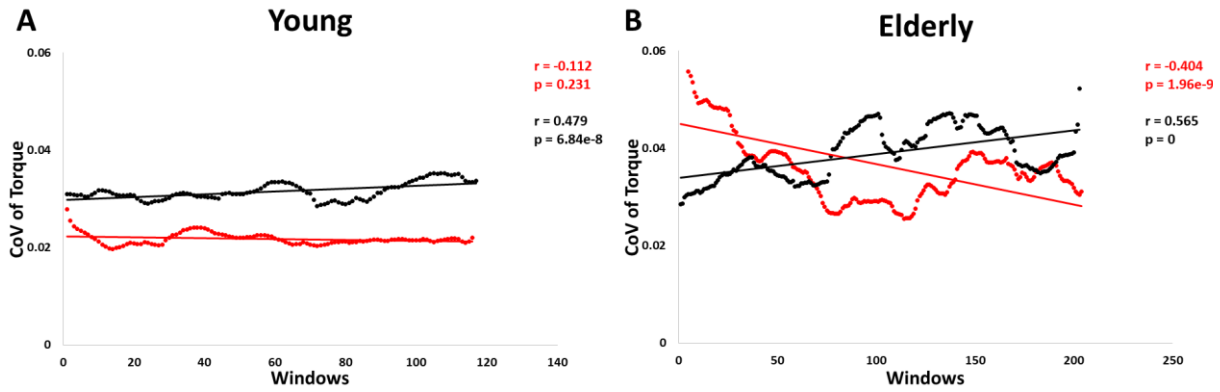

Figure 14: Scatter plot of the average CoV of Torque and windows (time) signal are shown for A) Young and B) Elderly participants. Associated r and p-values are calculated using Spearman's rank correlation. Correlations calculated for the first 25% of the contraction (red) and the last 25% of the contraction (black) prior to task failure.

5. Discussion

Summary of Key Findings

I. Significant differences in intramuscular coherence existed between pre- and post-fatigue conditions in the alpha and beta bands of the young group using the LA filter. No such differences were found in any of the frequency bands in the elderly.

II. Significant positive correlations appeared between the intramuscular coherence calculated in the alpha band and the CoV of torque for both young and elderly groups.

III. Significant negative correlations existed between the intramuscular coherence calculated in the beta/gamma bands and the CoV of torque for the young group. Differing from the significant positive correlations seen in the elderly group between the beta/gamma bands and the CoV of torque.

5.1. Time-Frequency Features

During submaximal fatiguing contractions, ARV and RMS gradually increased while MDF and MNF decreased for all subjects in both young and elderly groups indicating development of muscle fatigue. This behaviour is seen in various studies on fatigue development in young [49], [105], and elderly [105]–[107]. Although features in both groups exhibit similar trends, it is generally argued that there are differences in fatigue development between the young and elderly. This is substantiated by the fact that morphological changes due to aging, such as a decreased number in type II muscle fibers and changes in metabolic activity such as a decrease in lactate dehydrogenase activity affect these features [108], [109]. In fact, Yamada et al. found that the decreasing rate of the MDF feature was significantly smaller in the elderly than that of the young [105]. Although the current study did find similar behaviour, no statistically significant differences were found. The discrepancies of the current results and reports in the literature can be attributed to different fatiguing protocols, where Yamada et al. utilized a different contraction duration and

intensity (60% MVC for 60 seconds) which can potentially lead to differences in excitatory and inhibitory spinal inputs to the motor neuron pool [110]. Another reason for the different observations is the fact that the study used female participants, who are known to be more resistant to fatigue than male [111], likely reduced the detectable age-related differences. In agreement with the results of this paper, a study conducted by Yassierli et al. found no difference between the young and elderly for sustained 30%,50% and 70% MVC shoulder abductions and torso extensions [106]. Both Bipolar and Laplacian spatial filters were applied to the sEMG signal to isolate motor units directly below the measuring site and reduce the amount of cross talk. However, this also revealed no significant differences between both groups, suggesting that these features are not robust enough to capture age-related differences in fatigue development.

5.2. Intramuscular Coherence

Intramuscular coherence was utilized as a more robust methodology to assess age-related differences in muscle fatigue development due to it ability to measure oscillatory drive to motor units during voluntary contractions. Pooled coherence can be understood as the linear summation of the synergistic component common to separate MUs as well as components of the neural drive unique to each MU [102]. When MP was applied, the resulting pooled coherence showed significantly high values across all physiologically relevant frequency bands regardless of age group, as seen in Figure 10. This can be attributed to the fact that two MP EMG signals from which the coherence is calculated share a significant amount of common MU activations, *i.e.*, significant crosstalk, resulting significant positive bias to the estimated coherence. Multiple studies have also reported crosstalk increasing coherence values, and it should be carefully considered as a confounding factor when calculating coherence [112]–[114]. BP filter had the advantage of reducing this crosstalk by subtracting two signals obtained from adjacent electrodes [115].

Similarly, LA filter also served to further reduce the crosstalk and enhance single MU activity through applying a weighted summation of surrounding electrodes [40]. Although both spatial filters greatly reduced the inflated coherence values in both groups, the BP filter reported coherence values consistently above the significance level for all frequencies, indicating that the reduction that BP had on crosstalk was insufficient. The coherence calculated from the LA filter seemingly reduced the coherence values, indicating it was able to filter out more crosstalk when compared to BP. This is in agreement with the literature [116].

Accordingly, the LA filter was the only configuration to find significant differences in mean coherence values between pre- and post-fatigue conditions, albeit only within the young population. In general, both populations exhibited an increase in mean coherence from pre to post fatigue for all frequency bands, but a significant difference was only recorded in the alpha and beta bands for the young population. This indicates that the young group underwent significant changes in corticospinal excitability during the fatiguing contraction; the elderly likely had similar neurophysiological change as indicated by the general increase in mean alpha and beta coherence, but significance changes was not detected in the current study. According to [117], the elderly experience a deficit in the activation of the corticomotoneuronal pathway which can potentially lead to a lesser increase in mean beta coherence after fatigue. The results of this study are in line with results from a previous study which observed increases in intramuscular coherence in the alpha and beta bands in the first dorsal interosseous and tibialis anterior muscle [8], [118]. However, the study regarding the tibialis anterior recorded no significant increase in beta band coherence which indicates that the changes in corticospinal pathways may be dependent on the muscle studied or the task performed.

Investigation of force variability revealed that there was a significantly positive correlation in the alpha band in both age groups as the contraction approached task failure. The physiological basis behind this phenomenon is that the neural drive responsible for generating the force is filtered by the average twitch of the MUs, causing higher frequencies to be attenuated and lower frequencies to be enhanced [118]. This is further substantiated by the fact that neural drive typically increases to maintain a constant force as the approaching task failure, resulting in a decrease in torque steadiness and increase in low-frequency coherence [85], [118]. In contrast to this study, significant correlation was observed in the higher frequency bands for both groups as the task approached failure. This was evidenced by the increase in both mean beta and gamma coherence observed as fatigue progressed. Although this correlation goes against previously established physiological phenomenon, it is inline with a recent study that questioned the linearity of the transformation of motoneuron pool inputs into force. If the transformation is truly linear, it suggests that high frequency input to the muscle will get filtered out and have no effect on force control. A simulation study conducted by Watanabe et al. suggested that an increasing beta and gamma band input to the motoneurons increased the steadiness of the force generated by the muscle [119]. They had associated the muscles response to the cortical oscillations to the recruitment strategies of spinal cord motoneurons[119]. These results are inline with the results seen in the young population, which observed a significant negative correlation was seen between torque variability and mean beta/gamma coherence prior to task failure. However, the elderly group showed significant positive correlations between torque variability and beta/gamma coherence. The contrast in these results can be attributed to the inability of elderly adults to regulate and coordinate common synaptic inputs onto spinal motoneurons [120]. As such, it can be

interpreted that increases in oscillatory input are unable to modulate recruitment strategies of spinal motoneurons thus being unable to reduce the amount of force variability as fatigue progresses.

5.3. Limitations

Regarding methodological factors, a limitation in this study is the small sample size, particularly in the elderly group. This stemmed from difficulties in recruiting participants satisfying the inclusion criteria from that age group. For example, many elderly participants that inquired about the study were excluded due to increased amounts of subcutaneous fat in the arm regions which adversely affects the sEMG signal. Another reason some of the elderly subjects were excluded was due to uncertainty they achieved fatigue before task failure, as indicated by negative trends in MDF. It is possible that these subjects grew tired of the protocol and failed the task prior to actual muscle fatigue onset. The effect of fatigue on maximal torque production was not investigated after the protocol, which could help verify the efficacy of the protocol in eliciting fatigue. Another limitation in this study was the protocol was not necessarily optimized for coherence calculation because the internal bandpass filter of the EMG-USB2 device was used to remove motion artifact. This limits the information one can extract from the lower frequency bands such as lower alpha and delta (0-5 Hz), both of which have been linked to force generation.

The observations made in this study have been under the assumption that changes in intramuscular coherence solely reflect changes in the oscillatory cortical and sub-cortical processes within the cortico-spinal pathway. However, evidence suggests that other common neural drives can contribute to coherence as well [121]. As the current study does not provide a measure of the corticomuscular coherence (CMC), there is insufficient information on how much other neural processes contribute to the intramuscular coherence results observed.

5.4. Future Work

Future studies should prioritize the recruitment of subjects in both age groups, although elderly should be prioritized more due to the higher exclusion rates as seen in this study. Similarly, recruitment of females should be considered in future studies as biological sex is known to have an effect on the physiological mechanisms behind fatigue generation such as differences in muscle fiber composition and activation of MUs from cortical/subcortical regions [122]. Future work should also assess the repeatability of the proposed coherence measures by having subjects repeat the protocol after a set amount of time. This work would further validate the robustness of the measures and raise confidence in using this in other clinical studies. CMC should also be evaluated in conjunction with the current methodology via EEG or MEG to quantify the contribution of other neural drives to the muscle as fatigue progresses [123].

Furthermore, more work should be done to validate the use of interference sEMG in the calculation of intramuscular coherence. Commonly in the literature, intramuscular coherence is calculated between motor unit spike trains found by sEMG decomposition techniques or intramuscular electrodes to get a more accurate representation of individual MUs throughout the contraction [8], [118]. However, this technique is invasive and computationally intensive, reducing the capability of this technology to be used outside of a clinical environment. Future studies should adopt one of these techniques in the protocol such that a correlation analysis can be performed. If correlation between intramuscular coherence calculated using interference sEMG signals and between MU's extracted from signal decomposition is found, not only will the robustness of the measure be increased, but the confidence in implementing this technology in future studies.

6. Conclusion

The following objectives were explored in this study:

I. The ability of different spatial filter electrode configurations to detect fatigue related differences in a) conventional EMG features and, b) mean coherence within and between the different age groups was evaluated. This revealed that spatial filters were not sensitive for conventionally used time-frequency domain features in muscle fatigue detection but was sensitive for calculating fatigue related changes in mean intramuscular coherence.

II. The evolution of force steadiness and mean coherence throughout the fatiguing contraction in each frequency band was examined. Significant correlations were noticed between mean intramuscular coherence in the alpha, beta, and gamma bands and force steadiness, particularly in the final 25% of the contraction.

III. Age-related differences in muscle fatigue generation existed when comparing the trend of intramuscular coherence in the beta and gamma bands with force steadiness.

Objective I was addressed revealing that the application of MP, BP, and LA spatial filters had no effect on conventional time-frequency domain features pre- and post-fatigue within and between both the young and elderly groups. However, differences between the mean coherence calculated pre- and post-fatigue were found in the alpha and beta bands within the young group using the LA filter. Objective II and III was completed and revealed that both the young and elderly have different trends in mean coherence as force steadiness decreases in response to fatigue. The young group was found to have a decreasing trend in mean beta and gamma coherence as force steadiness decreased whereas the elderly was found to have an increase, demonstrating possible age-related changes in MU recruitment strategies.

This work is one of the first studies to assess the utility of different spatial filters on the calculation of intramuscular coherence using interference sEMG signals. Furthermore, this work provides an original methodology of calculating coherence through pooling together coherence found between different electrode pairs within the HD-sEMG grid. Moreover, this study presents novel findings that MUs within the young and elderly have different responses to fatigue related changes in oscillatory input as characterized by force steadiness.

References

[1] S. D. Mair, A. V Seaber, R. R. Glisson, and W. E. J. Garrett, “The role of fatigue in susceptibility to acute muscle strain injury.,” *Am. J. Sports Med.*, vol. 24, no. 2, pp. 137–143, 1996, doi: 10.1177/036354659602400203.

[2] D. Mori *et al.*, “Measurement of Low Back Muscle Fatigue and Recovery Time During and After Isometric Endurance Test,” vol. 489, 2016, pp. 297–308.

[3] J. A. Faulkner, S. V Brooks, and E. Zerba, “Muscle atrophy and weakness with aging: contraction-induced injury as an underlying mechanism.,” *J. Gerontol. A. Biol. Sci. Med. Sci.*, vol. 50 Spec No, pp. 124–129, Nov. 1995, doi: 10.1093/gerona/50a.special_issue.124.

[4] J. Lexell, “Human aging, muscle mass, and fiber type composition. J Gerontol A Biol Sci Med Sci,” *J. Gerontol. A. Biol. Sci. Med. Sci.*, vol. 50 Spec No, pp. 11–16, Dec. 1995, doi: 10.1093/gerona/50A.Special_Issue.11.

[5] M. Cifrek, V. Medved, S. Tonkovic, and S. Ostojić, “Surface EMG Based Muscle Fatigue Evaluation in Biomechanics,” *Clin. Biomech. (Bristol, Avon)*, vol. 24, pp. 327–340, Jun. 2009, doi: 10.1016/j.clinbiomech.2009.01.010.

[6] M. Rojas-Martínez, L. Y. Serna, M. Jordanic, H. R. Marateb, R. Merletti, and M. Á. Mañanas, “High-density surface electromyography signals during isometric contractions of elbow muscles of healthy humans,” *Sci. Data*, vol. 7, no. 1, p. 397, 2020, doi: 10.1038/s41597-020-00717-6.

[7] S. Gandevia, “Spinal and Supraspinal Factors in Human Muscle Fatigue,” *Physiol. Rev.*,

vol. 81, pp. 1725–1789, Nov. 2001, doi: 10.1152/physrev.2001.81.4.1725.

[8] L. McManus, X. Hu, W. Z. Rymer, N. L. Suresh, and M. M. Lowery, "Muscle fatigue increases beta-band coherence between the firing times of simultaneously active motor units in the first dorsal interosseous muscle.," *J. Neurophysiol.*, vol. 115, no. 6, pp. 2830–2839, Jun. 2016, doi: 10.1152/jn.00097.2016.

[9] "Functions of the Musculoskeletal System." [Online]. Available: https://bio.libretexts.org/@go/page/13988.

[10] V. M. Dave HD, Shook M, "Anatomy, Skeletal Muscle.," in *StatPearls [Internet]*, Treasure Island (FL): StatPearls Publishing;, 2021.

[11] L. M. B. S. D. A. H. R. H. J. K. M. L. P. M. K. M.-G. D. Q. and J. Runyeon, *Anatomy and Physiology*. OpenStax/Oregon State University, 2021.

[12] E. M. Noto RE, Leavitt L, *Physiology, Muscle*. Treasure Island (FL): StatPearls Publishing, 2021.

[13] J. Feher, "3.4 - Skeletal Muscle Mechanics," J. B. T.-Q. H. P. Feher, Ed. Boston: Academic Press, 2012, pp. 239–248.

[14] M. Beretta-Piccoli *et al.*, "Evaluation of central and peripheral fatigue in the quadriceps using fractal dimension and conduction velocity in young females.," *PLoS One*, vol. 10, no. 4, p. e0123921, 2015, doi: 10.1371/journal.pone.0123921.

[15] D. G. Allen, G. D. Lamb, and H. Westerblad, "Skeletal Muscle Fatigue: Cellular Mechanisms," *Physiol. Rev.*, vol. 88, no. 1, pp. 287–332, Jan. 2008, doi: 10.1152/physrev.00015.2007.

[16] J. L. Taylor, M. Amann, J. Duchateau, R. Meeusen, and C. L. Rice, “Neural Contributions to Muscle Fatigue: From the Brain to the Muscle and Back Again,” *Med. Sci. Sports Exerc.*, vol. 48, no. 11, pp. 2294–2306, Nov. 2016, doi: 10.1249/MSS.0000000000000923.

[17] J. Wan, Z. Qin, P. Wang, Y. Sun, and X. Liu, “Muscle fatigue: General understanding and treatment,” *Exp. Mol. Med.*, vol. 49, p. e384, Oct. 2017, doi: 10.1038/emm.2017.194.

[18] J. Laurin, V. Pertici, E. Dousset, T. Marqueste, and P. Decherchi, “Group III and IV Muscle Afferents: Role on Central Motor Drive and Clinical Implications,” *Neuroscience*, vol. 290, Feb. 2015, doi: 10.1016/j.neuroscience.2015.01.065.

[19] A. Zając, M. Chalimoniuk, A. Maszczyk, A. Gołaś, and J. Lngfort, “Central and Peripheral Fatigue During Resistance Exercise - A Critical Review,” *J. Hum. Kinet.*, vol. 49, pp. 159–169, Dec. 2015, doi: 10.1515/hukin-2015-0118.

[20] E. Cè, S. Longo, E. Limonta, G. Coratella, S. Rampichini, and F. Esposito, “Peripheral fatigue: new mechanistic insights from recent technologies,” *Eur. J. Appl. Physiol.*, vol. 120, no. 1, pp. 17–39, 2020, doi: 10.1007/s00421-019-04264-w.

[21] V. Santilli, A. Bernetti, M. Mangone, and M. Paoloni, “Clinical definition of sarcopenia.,” *Clin. cases Miner. bone Metab. Off. J. Ital. Soc. Osteoporosis, Miner. Metab. Skelet. Dis.*, vol. 11, no. 3, pp. 177–180, Sep. 2014.

[22] S. von Haehling, J. E. Morley, and S. D. Anker, “An overview of sarcopenia: facts and numbers on prevalence and clinical impact,” *J. Cachexia. Sarcopenia Muscle*, vol. 1, no. 2, pp. 129–133, Dec. 2010, doi: 10.1007/s13539-010-0014-2.

[23] C. S. Klein, G. D. Marsh, R. J. Petrella, and C. L. Rice, “Muscle fiber number in the biceps brachii muscle of young and old men,” *Muscle Nerve*, vol. 28, no. 1, pp. 62–68, Jul. 2003, doi: https://doi.org/10.1002/mus.10386.

[24] J. Lexell, C. C. Taylor, and M. Sjöström, “What is the cause of the ageing atrophy? Total number, size and proportion of different fiber types studied in whole vastus lateralis muscle from 15- to 83-year-old men.,” *J. Neurol. Sci.*, vol. 84, no. 2–3, pp. 275–294, Apr. 1988, doi: 10.1016/0022-510x(88)90132-3.

[25] J. A. Kent-Braun, “Skeletal muscle fatigue in old age: whose advantage?,” *Exerc. Sport Sci. Rev.*, vol. 37, no. 1, pp. 3–9, Jan. 2009, doi: 10.1097/JES.0b013e318190ea2e.

[26] S. Rubinstein and G. Kamen, “Decreases in motor unit firing rate during sustained maximal-effort contractions in young and older adults.,” *J. Electromyogr. Kinesiol. Off. J. Int. Soc. Electrophysiol. Kinesiol.*, vol. 15, no. 6, pp. 536–543, Dec. 2005, doi: 10.1016/j.jelekin.2005.04.001.

[27] D. W. Russ, T. F. Towse, D. M. Wigmore, I. R. Lanza, and J. A. Kent-Braun, “Contrasting influences of age and sex on muscle fatigue.,” *Med. Sci. Sports Exerc.*, vol. 40, no. 2, pp. 234–241, Feb. 2008, doi: 10.1249/mss.0b013e31815bbb93.

[28] K. G. Avin and L. A. F. Law, “Age-related differences in muscle fatigue vary by contraction type: a meta-analysis,” *Phys. Ther.*, vol. 91, no. 8, pp. 1153–1165, Aug. 2011, doi: 10.2522/ptj.20100333.

[29] S. K. Hunter, A. Critchlow, and R. M. Enoka, “Influence of aging on sex differences in muscle fatigability,” *J. Appl. Physiol.*, vol. 97, no. 5, pp. 1723–1732, Nov. 2004, doi: 10.1152/japplphysiol.00460.2004.

[30] S. K. Hunter, A. Critchlow, and R. M. Enoka, “Muscle endurance is greater for old men compared with strength-matched young men.,” *J. Appl. Physiol.*, vol. 99, no. 3, pp. 890–897, Sep. 2005, doi: 10.1152/japplphysiol.00243.2005.

[31] C. J. McNeil and C. L. Rice, “Fatigability is increased with age during velocity-dependent contractions of the dorsiflexors.,” *J. Gerontol. A. Biol. Sci. Med. Sci.*, vol. 62, no. 6, pp. 624–629, Jun. 2007, doi: 10.1093/gerona/62.6.624.

[32] S. Baudry, M. Klass, B. Pasquet, and J. Duchateau, “Age-related fatigability of the ankle dorsiflexor muscles during concentric and eccentric contractions.,” *Eur. J. Appl. Physiol.*, vol. 100, no. 5, pp. 515–525, Jul. 2007, doi: 10.1007/s00421-006-0206-9.

[33] U. Granacher, M. Gruber, D. Förderer, D. Strass, and A. Gollhofer, “Effects of ankle fatigue on functional reflex activity during gait perturbations in young and elderly men,” *Gait Posture*, vol. 32, no. 1, pp. 107–112, 2010, doi: https://doi.org/10.1016/j.gaitpost.2010.03.016.

[34] N. Nazmi, M. A. Abdul Rahman, S.-I. Yamamoto, S. A. Ahmad, H. Zamzuri, and S. A. Mazlan, “A Review of Classification Techniques of EMG Signals during Isotonic and Isometric Contractions.,” *Sensors (Basel).*, vol. 16, no. 8, Aug. 2016, doi: 10.3390/s16081304.

[35] L. Shaw and S. Bhaga, “Online EMG Signal Analysis for diagnosis of Neuromuscular diseases by using PCA and PNN.,” *Int. J. Eng. Sci. Technol. 0975-5462*, vol. 4, pp. 4453–4459, Oct. 2012.

[36] B. Afsharipour, S. Soedirdjo, and R. Merletti, “Two-dimensional surface EMG: The effects of electrode size, interelectrode distance and image truncation,” *Biomed. Signal*

Process. Control, vol. 49, pp. 298–307, 2019, doi: https://doi.org/10.1016/j.bspc.2018.12.001.

[37] U. Kuruganti, A. Pradhan, and J. Toner, "High-Density Electromyography Provides Improved Understanding of Muscle Function for Those With Amputation ," *Frontiers in Medical Technology* , vol. 3. p. 41, 2021, [Online]. Available: https://www.frontiersin.org/article/10.3389/fmedt.2021.690285.

[38] L. Mesin, "Crosstalk in surface electromyogram: literature review and some insights.," *Phys. Eng. Sci. Med.*, vol. 43, no. 2, pp. 481–492, Jun. 2020, doi: 10.1007/s13246-020-00868-1.

[39] X. Zhang, X. Li, X. Tang, X. Chen, X. Chen, and P. Zhou, "Spatial filtering for enhanced high-density surface electromyographic examination of neuromuscular changes and its application to spinal cord injury," *J. Neuroeng. Rehabil.*, vol. 17, no. 1, p. 160, 2020, doi: 10.1186/s12984-020-00786-z.

[40] K. Ollivier, P. Portero, O. Maïsetti, and J.-Y. Hogrel, "Repeatability of surface EMG parameters at various isometric contraction levels and during fatigue using bipolar and Laplacian electrode configurations," *J. Electromyogr. Kinesiol.*, vol. 15, no. 5, pp. 466–473, 2005, doi: https://doi.org/10.1016/j.jelekin.2005.01.004.

[41] C. Disselhorst-Klug, J. Bahm, V. Ramaekers, A. Trachterna, and G. Rau, "Non-invasive approach of motor unit recording during muscle contractions in humans.," *Eur. J. Appl. Physiol.*, vol. 83, no. 2–3, pp. 144–150, Oct. 2000, doi: 10.1007/s004210000272.

[42] J. Kilby, K. Prasad, and G. Mawston, "Multi-Channel Surface Electromyography Electrodes: A Review," *IEEE Sens. J.*, vol. 16, no. 14, pp. 5510–5519, 2016, doi:

10.1109/JSEN.2016.2569072.

[43] R. Merletti and S. Muceli, “Tutorial. Surface EMG detection in space and time: Best practices,” *J. Electromyogr. Kinesiol.*, vol. 49, p. 102363, 2019, doi: https://doi.org/10.1016/j.jelekin.2019.102363.

[44] L. Xu, C. Rabotti, and M. Mischi, “Towards Real-Time Estimation of Muscle-Fiber Conduction Velocity Using Delay-Locked Loop,” *IEEE Trans. Neural Syst. Rehabil. Eng.*, vol. PP, p. 1, Nov. 2016, doi: 10.1109/TNSRE.2016.2632755.

[45] R. Merletti, T. Vieira, and D. Farina, “Techniques for Information Extraction from the Surface EMG Signalhigh-Density Surface EMG,” in *Surface Electromyography: Physiology, Engineering and Applications*, 2016, pp. 126–157.

[46] D. Farina, D. F. Stegeman, and R. Merletti, “Biophysics of the Generation of EMG Signals,” *Surface Electromyography : Physiology, Engineering, and Applications*. pp. 1–24, Apr. 22, 2016, doi: https://doi.org/10.1002/9781119082934.ch02.

[47] Y. Fukuoka *et al.*, “Development of a Compact Wireless Laplacian Electrode Module for Electromyograms and Its Human Interface Applications,” *Sensors* , vol. 13, no. 2. 2013, doi: 10.3390/s130202368.

[48] J. H. Viitasalo and P. V Komi, “Signal characteristics of EMG during fatigue.,” *Eur. J. Appl. Physiol. Occup. Physiol.*, vol. 37, no. 2, pp. 111–121, Sep. 1977, doi: 10.1007/BF00421697.

[49] M. Al-mulla, F. Sepulveda, and M. Colley, “sEMG Techniques to Detect and Predict Localised Muscle Fatigue,” in *EMG Methods for Evaluating Muscle and Nerve Function,*

2012.

[50] J. B. Fernando, M. Yoshioka, and J. Ozawa, “Estimation of muscle fatigue by ratio of mean frequency to average rectified value from surface electromyography.,” *Annu. Int. Conf. IEEE Eng. Med. Biol. Soc. IEEE Eng. Med. Biol. Soc. Annu. Int. Conf.*, vol. 2016, pp. 5303–5306, Aug. 2016, doi: 10.1109/EMBC.2016.7591924.

[51] G. Kim, M. A. Ahad, M. Ferdjallah, and G. F. Harris, “Correlation of muscle fatigue indices between intramuscular and surface EMG signals,” in *Proceedings 2007 IEEE SoutheastCon*, 2007, pp. 378–382, doi: 10.1109/SECON.2007.342928.

[52] M. R. Al-Mulla, F. Sepulveda, and M. Colley, “A review of non-invasive techniques to detect and predict localised muscle fatigue,” *Sensors*, vol. 11, no. 4, pp. 3545–3594, 2011, doi: 10.3390/s110403545.

[53] G. Zhang, E. Morin, Y. Zhang, and S. A. Etemad, “Non-invasive detection of low-level muscle fatigue using surface EMG with wavelet decomposition.,” *Annu. Int. Conf. IEEE Eng. Med. Biol. Soc. IEEE Eng. Med. Biol. Soc. Annu. Int. Conf.*, vol. 2018, pp. 5648–5651, Jul. 2018, doi: 10.1109/EMBC.2018.8513588.

[54] S. Xiao and S. C. Leung, “Muscle fatigue monitoring using wavelet decomposition of surface EMG.,” *Biomed. Sci. Instrum.*, vol. 34, pp. 147–152, 1997.

[55] B. Idrees and O. Farooq, *Estimation of muscle fatigue using wavelet decomposition*. 2015.

[56] D. Farina and F. Negro, “Common synaptic input to motor neurons, motor unit synchronization, and force control.,” *Exerc. Sport Sci. Rev.*, vol. 43, no. 1, pp. 23–33, Jan. 2015, doi: 10.1249/JES.0000000000000032.

[57] L.-J. Wang *et al.*, “Muscle Fatigue Enhance Beta Band EMG-EMG Coupling of Antagonistic Muscles in Patients With Post-stroke Spasticity,” *Front. Bioeng. Biotechnol.*, vol. 8, p. 1007, Aug. 2020, doi: 10.3389/fbioe.2020.01007.

[58] E. H. F. van Asseldonk, S. F. Campfens, S. J. F. Verwer, M. J. A. M. van Putten, and D. F. Stegeman, “Reliability and agreement of intramuscular coherence in tibialis anterior muscle,” *PLoS One*, vol. 9, no. 2, pp. e88428–e88428, Feb. 2014, doi: 10.1371/journal.pone.0088428.

[59] C. M. Laine and F. J. Valero-Cuevas, “Intermuscular coherence reflects functional coordination,” *J. Neurophysiol.*, vol. 118, no. 3, pp. 1775–1783, Jun. 2017, doi: 10.1152/jn.00204.2017.

[60] J. M. Kilner, S. N. Baker, S. Salenius, V. Jousmäki, R. Hari, and R. N. Lemon, “Task-dependent modulation of 15-30 Hz coherence between rectified EMGs from human hand and forearm muscles,” *J. Physiol.*, vol. 516 (Pt 2, no. Pt 2, pp. 559–570, Apr. 1999, doi: 10.1111/j.1469-7793.1999.0559v.x.

[61] C. J. De Luca and Z. Erim, “Common Drive in Motor Units of a Synergistic Muscle Pair,” *J. Neurophysiol.*, vol. 87, no. 4, pp. 2200–2204, Apr. 2002, doi: 10.1152/jn.00793.2001.

[62] M. E. Spedden, J. B. Nielsen, and S. S. Geertsen, “Oscillatory Corticospinal Activity during Static Contraction of Ankle Muscles Is Reduced in Healthy Old versus Young Adults,” *Neural Plast.*, vol. 2018, p. 3432649, Apr. 2018, doi: 10.1155/2018/3432649.

[63] C. M. Laine and F. J. Valero-Cuevas, “Parkinson’s Disease Exhibits Amplified Intermuscular Coherence During Dynamic Voluntary Action ,” *Frontiers in Neurology* , vol. 11. p. 204, 2020, [Online]. Available:

https://www.frontiersin.org/article/10.3389/fneur.2020.00204.

[64] S. Hansen, N. L. Hansen, L. O. D. Christensen, N. T. Petersen, and J. B. Nielsen, "Coupling of antagonistic ankle muscles during co-contraction in humans.," *Exp. brain Res.*, vol. 146, no. 3, pp. 282–292, Oct. 2002, doi: 10.1007/s00221-002-1152-3.

[65] C. De Marchis, G. Severini, A. M. Castronovo, M. Schmid, and S. Conforto, "Intermuscular coherence contributions in synergistic muscles during pedaling.," *Exp. brain Res.*, vol. 233, no. 6, pp. 1907–1919, Jun. 2015, doi: 10.1007/s00221-015-4262-4.

[66] S. Kattla and M. M. Lowery, "Fatigue related changes in electromyographic coherence between synergistic hand muscles.," *Exp. brain Res.*, vol. 202, no. 1, pp. 89–99, Apr. 2010, doi: 10.1007/s00221-009-2110-0.

[67] Y.-J. Chang *et al.*, "Increases of quadriceps inter-muscular cross-correlation and coherence during exhausting stepping exercise," *Sensors (Basel).*, vol. 12, no. 12, pp. 16353–16367, Nov. 2012, doi: 10.3390/s121216353.

[68] L. Wang, A. Lu, S. Zhang, W. Niu, F. Zheng, and M. Gong, "Fatigue-related electromyographic coherence and phase synchronization analysis between antagonistic elbow muscles," *Exp. Brain Res.*, vol. 233, no. 3, pp. 971–982, 2015, doi: 10.1007/s00221-014-4172-x.

[69] A. Danna-Dos Santos, B. Poston, M. Jesunathadas, L. R. Bobich, T. M. Hamm, and M. Santello, "Influence of fatigue on hand muscle coordination and EMG-EMG coherence during three-digit grasping," *J. Neurophysiol.*, vol. 104, no. 6, pp. 3576–3587, Dec. 2010, doi: 10.1152/jn.00583.2010.

[70] P. C. R. dos Santos, C. J. C. Lamoth, F. A. Barbieri, I. Zijdewind, L. T. B. Gobbi, and T. Hortobágyi, “Age-specific modulation of intermuscular beta coherence during gait before and after experimentally induced fatigue,” *Sci. Rep.*, vol. 10, no. 1, p. 15854, 2020, doi: 10.1038/s41598-020-72839-1.

[71] T. W. Boonstra *et al.*, “Fatigue-related changes in motor-unit synchronization of quadriceps muscles within and across legs.,” *J. Electromyogr. Kinesiol. Off. J. Int. Soc. Electrophysiol. Kinesiol.*, vol. 18, no. 5, pp. 717–731, Oct. 2008, doi: 10.1016/j.jelekin.2007.03.005.

[72] J. G. Semmler, S. A. Ebert, and J. Amarasena, “Eccentric muscle damage increases intermuscular coherence during a fatiguing isometric contraction,” *Acta Physiol.*, vol. 208, no. 4, pp. 362–375, Aug. 2013, doi: https://doi.org/10.1111/apha.12111.

[73] T. Watanabe, K. Saito, K. Ishida, S. Tanabe, and I. Nojima, “Fatigue-induced decline in low-frequency common input to bilateral and unilateral plantar flexors during quiet standing,” *Neurosci. Lett.*, vol. 686, pp. 193–197, 2018, doi: https://doi.org/10.1016/j.neulet.2018.09.019.

[74] I.-S. Hwang, Y.-T. Lin, C.-C. Huang, and Y.-C. Chen, “Fatigue-related modulation of low-frequency common drive to motor units,” *Eur. J. Appl. Physiol.*, vol. 120, no. 6, pp. 1305–1317, 2020, doi: 10.1007/s00421-020-04363-z.

[75] T. J. Dartnall, M. A. Nordstrom, and J. G. Semmler, “Motor unit synchronization is increased in biceps brachii after exercise-induced damage to elbow flexor muscles.,” *J. Neurophysiol.*, vol. 99, no. 2, pp. 1008–1019, Feb. 2008, doi: 10.1152/jn.00686.2007.

[76] X. Liu and M. Zhou, “Muscle Fatigue Monitoring: Using HD-sEMG Techniques BT -

Human Interaction, Emerging Technologies and Future Applications II," 2020, pp. 551–556.

[77] R. Merletti, M. Knaflitz, and C. J. De Luca, "Myoelectric manifestations of fatigue in voluntary and electrically elicited contractions.," *J. Appl. Physiol.*, vol. 69, no. 5, pp. 1810–1820, Nov. 1990, doi: 10.1152/jappl.1990.69.5.1810.

[78] M. Hagberg, "Work load and fatigue in repetitive arm elevations.," *Ergonomics*, vol. 24, no. 7, pp. 543–555, Jul. 1981, doi: 10.1080/00140138108924875.

[79] G. Marco, B. Alberto, and V. Taian, "Surface EMG and muscle fatigue: multi-channel approaches to the study of myoelectric manifestations of muscle fatigue.," *Physiol. Meas.*, vol. 38, no. 5, pp. R27–R60, May 2017, doi: 10.1088/1361-6579/aa60b9.

[80] R. Merletti, L. R. Lo Conte, and C. Orizio, "Indices of muscle fatigue.," *J. Electromyogr. Kinesiol. Off. J. Int. Soc. Electrophysiol. Kinesiol.*, vol. 1, no. 1, pp. 20–33, 1991, doi: 10.1016/1050-6411(91)90023-X.

[81] G. M. Hägg, "Interpretation of EMG spectral alterations and alteration indexes at sustained contraction.," *J. Appl. Physiol.*, vol. 73, no. 4, pp. 1211–1217, Oct. 1992, doi: 10.1152/jappl.1992.73.4.1211.

[82] Biodex Medical Systems Inc, "Biodex Multi-Joint System – Pro. Setup/Operation Manual." Shirley, [Online]. Available: https://umanitoba.ca/faculties/kinrec/media/Biodex_hardware.pdf.

[83] C. M. Germer, D. Farina, L. A. Elias, S. Nuccio, F. Hug, and A. Del Vecchio, "Surface EMG cross talk quantified at the motor unit population level for muscles of the hand,

thigh, and calf," *J. Appl. Physiol.*, vol. 131, no. 2, pp. 808–820, Jul. 2021, doi: 10.1152/japplphysiol.01041.2020.

[84] W.-Y. Hsu, Y.-C. Li, C.-Y. Hsu, C.-T. Liu, and H.-W. Chiu, "Application of multiscale amplitude modulation features and fuzzy C-means to brain-computer interface.," *Clin. EEG Neurosci.*, vol. 43, no. 1, pp. 32–38, Jan. 2012, doi: 10.1177/1550059411429528.

[85] P. Contessa, A. Adam, and C. J. De Luca, "Motor unit control and force fluctuation during fatigue," *J. Appl. Physiol.*, vol. 107, no. 1, pp. 235–243, Jul. 2009, doi: 10.1152/japplphysiol.00035.2009.

[86] S. Gottlieb and O. C. Lippold, "The 4-6 HZ tremor during sustained contraction in normal human subjects," *J. Physiol.*, vol. 336, pp. 499–509, Mar. 1983, doi: 10.1113/jphysiol.1983.sp014594.

[87] O. Missenard, D. Mottet, and S. Perrey, "Factors responsible for force steadiness impairment with fatigue.," *Muscle Nerve*, vol. 40, no. 6, pp. 1019–1032, Dec. 2009, doi: 10.1002/mus.21331.

[88] B. L. Tracy and R. M. Enoka, "Older adults are less steady during submaximal isometric contractions with the knee extensor muscles.," *J. Appl. Physiol.*, vol. 92, no. 3, pp. 1004–1012, Mar. 2002, doi: 10.1152/japplphysiol.00954.2001.

[89] S. K. Hunter, G. Todd, J. E. Butler, S. C. Gandevia, and J. L. Taylor, "Recovery from supraspinal fatigue is slowed in old adults after fatiguing maximal isometric contractions," *J. Appl. Physiol.*, vol. 105, no. 4, pp. 1199–1209, Oct. 2008, doi: 10.1152/japplphysiol.01246.2007.

[90] T. J. Doherty, “Invited Review: Aging and sarcopenia,” *J. Appl. Physiol.*, vol. 95, no. 4, pp. 1717–1727, Oct. 2003, doi: 10.1152/japplphysiol.00347.2003.

[91] B. K. Barry, M. A. Pascoe, M. Jesunathadas, and R. M. Enoka, “Rate Coding Is Compressed But Variability Is Unaltered for Motor Units in a Hand Muscle of Old Adults,” *J. Neurophysiol.*, vol. 97, no. 5, pp. 3206–3218, May 2007, doi: 10.1152/jn.01280.2006.

[92] M. L. Vanden Noven, H. M. Pereira, T. Yoon, A. A. Stevens, K. A. Nielson, and S. K. Hunter, “Motor Variability during Sustained Contractions Increases with Cognitive Demand in Older Adults ,” *Frontiers in Aging Neuroscience* , vol. 6. p. 97, 2014, [Online]. Available: https://www.frontiersin.org/article/10.3389/fnagi.2014.00097.

[93] B. Yao, S. Salenius, G. H. Yue, R. W. Brown, and J. Z. Liu, “Effects of surface EMG rectification on power and coherence analyses: an EEG and MEG study.,” *J. Neurosci. Methods*, vol. 159, no. 2, pp. 215–223, Jan. 2007, doi: 10.1016/j.jneumeth.2006.07.008.

[94] M. E. Héroux and S. C. Gandevia, “Human muscle fatigue, eccentric damage and coherence in the EMG,” *Acta Physiol.*, vol. 208, no. 4, pp. 294–295, Aug. 2013, doi: https://doi.org/10.1111/apha.12133.

[95] D. Farina, F. Negro, and N. Jiang, “Identification of common synaptic inputs to motor neurons from the rectified electromyogram.,” *J. Physiol.*, vol. 591, no. 10, pp. 2403–2418, May 2013, doi: 10.1113/jphysiol.2012.246082.

[96] K. G. Keenan, D. Farina, K. S. Maluf, R. Merletti, and R. M. Enoka, “Influence of amplitude cancellation on the simulated surface electromyogram.,” *J. Appl. Physiol.*, vol. 98, no. 1, pp. 120–131, Jan. 2005, doi: 10.1152/japplphysiol.00894.2004.

[97] D. M. Halliday, J. R. Rosenberg, A. M. Amjad, P. Breeze, B. A. Conway, and S. F. Farmer, “A framework for the analysis of mixed time series/point process data--theory and application to the study of physiological tremor, single motor unit discharges and electromyograms.,” *Prog. Biophys. Mol. Biol.*, vol. 64, no. 2–3, pp. 237–278, 1995, doi: 10.1016/s0079-6107(96)00009-0.

[98] S. F. Farmer, F. D. Bremner, D. M. Halliday, J. R. Rosenberg, and J. A. Stephens, “The frequency content of common synaptic inputs to motoneurones studied during voluntary isometric contraction in man,” *J. Physiol.*, vol. 470, pp. 127–155, Oct. 1993, doi: 10.1113/jphysiol.1993.sp019851.

[99] A. M. Amjad, D. M. Halliday, J. R. Rosenberg, and B. A. Conway, “An extended difference of coherence test for comparing and combining several independent coherence estimates: theory and application to the study of motor units and physiological tremor.,” *J. Neurosci. Methods*, vol. 73, no. 1, pp. 69–79, Apr. 1997, doi: 10.1016/s0165-0270(96)02214-5.

[100] D. M. Halliday and J. R. Rosenberg, “On the application, estimation and interpretation of coherence and pooled coherence.,” *Journal of neuroscience methods*, vol. 100, no. 1–2. Netherlands, pp. 173–174, Jul. 2000, doi: 10.1016/s0165-0270(00)00267-3.

[101] J. R. Rosenberg, A. M. Amjad, P. Breeze, D. R. Brillinger, and D. M. Halliday, “The Fourier approach to the identification of functional coupling between neuronal spike trains.,” *Prog. Biophys. Mol. Biol.*, vol. 53, no. 1, pp. 1–31, 1989, doi: 10.1016/0079-6107(89)90004-7.

[102] M. Castronovo, C. De Marchis, M. Schmid, S. Conforto, and G. Severini, “Effect of Task

Failure on Intermuscular Coherence Measures in Synergistic Muscles," *Appl. Bionics Biomech.*, vol. 2018, Jun. 2018, doi: 10.1155/2018/4759232.

[103] R. Merletti, M. Knaflitz, and C. J. De Luca, "Myoelectric manifestations of fatigue in voluntary and electrically elicited contractions," *J. Appl. Physiol.*, vol. 69, no. 5, pp. 1810–1820, 1990, doi: 10.1152/jappl.1990.69.5.1810.

[104] H. Daanen, M. Mazure, M. Holewijn, and E. Velde, "Reproducibility of the mean power frequency of the surface electromyogram," *Eur. J. Appl. Physiol. Occup. Physiol.*, vol. 61, pp. 274–277, Feb. 1990, doi: 10.1007/BF00357612.

[105] H. Yamada *et al.*, "Effects of aging on EMG variables during fatiguing isometric contractions," *J. Hum. Ergol. (Tokyo).*, vol. 29, pp. 7–14, Dec. 2000.

[106] Yassierli, M. A. Nussbaum, H. Iridiastadi, and L. A. Wojcik, "The influence of age on isometric endurance and fatigue is muscle dependent: a study of shoulder abduction and torso extension," *Ergonomics*, vol. 50, no. 1, pp. 26–45, Jan. 2007, doi: 10.1080/00140130600967323.

[107] Y. Hara, T. W. Findley, A. Sugimoto, and K. Hanayama, "Muscle fiber conduction velocity (MFCV) after fatigue in elderly subjects," *Electromyogr. Clin. Neurophysiol.*, vol. 38, no. 7, pp. 427–435, 1998, [Online]. Available: http://europepmc.org/abstract/MED/9809231.

[108] O. Pastoris *et al.*, "The effects of aging on enzyme activities and metabolite concentrations in skeletal muscle from sedentary male and female subjects.," *Exp. Gerontol.*, vol. 35, no. 1, pp. 95–104, Feb. 2000, doi: 10.1016/s0531-5565(99)00077-7.

[109] P. V Komi and P. Tesch, “EMG frequency spectrum, muscle structure, and fatigue during dynamic contractions in man.,” *Eur. J. Appl. Physiol. Occup. Physiol.*, vol. 42, no. 1, pp. 41–50, Sep. 1979, doi: 10.1007/BF00421103.

[110] S. K. Hunter, J. Duchateau, and R. M. Enoka, “Muscle fatigue and the mechanisms of task failure.,” *Exerc. Sport Sci. Rev.*, vol. 32, no. 2, pp. 44–49, Apr. 2004, doi: 10.1097/00003677-200404000-00002.

[111] A. L. Hicks, J. Kent-Braun, and D. S. Ditor, “Sex Differences in Human Skeletal Muscle Fatigue,” *Exerc. Sport Sci. Rev.*, vol. 29, no. 3, 2001, [Online]. Available: https://journals.lww.com/acsm-essr/Fulltext/2001/07000/Sex_Differences_in_Human_Skeletal_Muscle_Fatigue.4.aspx.

[112] M. Mohr, T. Schön, V. von Tscharner, and B. M. Nigg, “Intermuscular Coherence Between Surface EMG Signals Is Higher for Monopolar Compared to Bipolar Electrode Configurations ,” *Frontiers in Physiology* , vol. 9. p. 566, 2018, [Online]. Available: https://www.frontiersin.org/article/10.3389/fphys.2018.00566.

[113] P. Grosse, M. J. Cassidy, and P. Brown, “EEG-EMG, MEG-EMG and EMG-EMG frequency analysis: physiological principles and clinical applications.,” *Clin. Neurophysiol. Off. J. Int. Fed. Clin. Neurophysiol.*, vol. 113, no. 10, pp. 1523–1531, Oct. 2002, doi: 10.1016/s1388-2457(02)00223-7.

[114] D. M. Halliday, B. A. Conway, L. O. D. Christensen, N. L. Hansen, N. P. Petersen, and J. B. Nielsen, “Functional coupling of motor units is modulated during walking in human subjects.,” *J. Neurophysiol.*, vol. 89, no. 2, pp. 960–968, Feb. 2003, doi: 10.1152/jn.00844.2002.

[115] A. Gallina, R. Merletti, and M. Gazzoni, “Innervation zone of the vastus medialis muscle: position and effect on surface EMG variables.,” *Physiol. Meas.*, vol. 34, no. 11, pp. 1411–1422, Nov. 2013, doi: 10.1088/0967-3334/34/11/1411.

[116] J. P. van Vugt and J. G. van Dijk, “A convenient method to reduce crosstalk in surface EMG. Cobb Award-winning article, 2001.,” *Clin. Neurophysiol. Off. J. Int. Fed. Clin. Neurophysiol.*, vol. 112, no. 4, pp. 583–592, Apr. 2001, doi: 10.1016/s1388-2457(01)00482-5.

[117] K. Chan, A. Raja, F. Strohschein, and K. Lechelt, “Age-Related Changes in Muscle Fatigue Resistance in Humans,” *Can. J. Neurol. Sci.*, vol. 27, pp. 220–228, Sep. 2000, doi: 10.1017/S0317167100000858.

[118] A. M. Castronovo, F. Negro, S. Conforto, and D. Farina, “The proportion of common synaptic input to motor neurons increases with an increase in net excitatory input,” *J. Appl. Physiol.*, vol. 119, no. 11, pp. 1337–1346, Sep. 2015, doi: 10.1152/japplphysiol.00255.2015.

[119] R. N. Watanabe and A. F. Kohn, “Fast Oscillatory Commands from the Motor Cortex Can Be Decoded by the Spinal Cord for Force Control,” *J. Neurosci.*, vol. 35, no. 40, pp. 13687–13697, Oct. 2015, doi: 10.1523/JNEUROSCI.1950-15.2015.

[120] S. K. Hunter, H. M. Pereira, and K. G. Keenan, “The aging neuromuscular system and motor performance,” *J. Appl. Physiol.*, vol. 121, no. 4, pp. 982–995, Oct. 2016, doi: 10.1152/japplphysiol.00475.2016.

[121] S. Sato and J. T. Choi, “Increased intramuscular coherence is associated with temporal gait symmetry during split-belt locomotor adaptation,” *J. Neurophysiol.*, vol. 122, no. 3,

pp. 1097–1109, Jul. 2019, doi: 10.1152/jn.00865.2018.

[122] S. K. Hunter, “Sex differences in human fatigability: mechanisms and insight to physiological responses,” *Acta Physiol. (Oxf).*, vol. 210, no. 4, pp. 768–789, Apr. 2014, doi: 10.1111/apha.12234.

[123] C. van de Steeg, A. Daffertshofer, D. F. Stegeman, and T. W. Boonstra, “High-density surface electromyography improves the identification of oscillatory synaptic inputs to motoneurons,” *J. Appl. Physiol.*, vol. 116, no. 10, pp. 1263–1271, Mar. 2014, doi: 10.1152/japplphysiol.01092.2013.

[124] H. Lim, I. Choi, S.-H. Hyun, H. Kim, and G. Lee, “Approaches to characterize the transcriptional trajectory of human myogenesis,” *Cell. Mol. Life Sci.*, vol. 78, pp. 1–14, May 2021, doi: 10.1007/s00018-021-03782-1.